GENETIC STRUCTURE AND CONNECTIVITY OF THE ENDANGERED GIANT KANGAROO RAT (*DIPODOMYS INGENS*) IN A HETEROGENEOUS ENVIRONMENT

By

Nathan Alexander

A Thesis Presented to

The Faculty of Humboldt State University

In Partial Fulfillment of the Requirements for the Degree

Master of Science in Natural Resources: Wildlife

Committee Membership

Dr. William “Tim” Bean, Committee Chair

Dr. Andrew Kinziger, Committee Member

Dr. Daniel Barton, Committee Member

Dr. Alison O’Dowd, Graduate Coordinator

December 2016

ABSTRACT

GENETIC STRUCTURE AND CONNECTIVITY OF THE EDNANGERED KANGAROO RAT (*DIPODOMYS* INGENS) IN A HETEROGENEOUS ENVIRONMENT

Nathan Alexander

Movement ecology and dispersal are important aspects of species' life histories that can inform conservation and management. Dispersal is often cryptic and difficult to detect, but recent advances genetic technology and applications have provided new approaches to identifying and describing dispersal patterns. Giant kangaroo rats (*Dipodomys ingens*) are an endangered heteromyid that appear to persist in small subpopulations in a heterogeneous environment of their northern range, the Ciervo-Panoche Natural Area, California. Previous work suggested high levels of genetic diversity between populations with genetic distances not being correlated to geographic distances. Here, I identified landscape population structure through clustering programs STRUCTURE and TESS, as well as a Moran Eigenvector Map. I identified straight-line geographic distance between related individuals using the program COLONY. Finally, I evaluated parameterization and combinations of hypothesized costs created from precipitation, slope, vegetation, and roads for Isolation by Resistance and least cost path using mantel and partial mantel tests. TESS and STRUCTURE identified 3-4 subpopulations, but this structure is most likely due to Isolation by Distance effects. I identified a full-sibling pair 5.52km apart. The best model suggested that straight-line geographic distance as well as slopes greater than 10 degrees negatively influenced dispersal. Conservation and de-listing of giant kangaroo rats will be dependent on habitat protection and creation rather than corridor protection.

Key Words: *Dipodomys ingens*, dispersal, gene flow, connectivity, landscape genetics

Contents

Table of Appendices

List of Tables

List of Figures

List of Appendices

Introduction

Dispersal is an informative and important aspect of understanding species' movement ecology, which informs our understanding of species persistence (Turchin 1998; Nathan 2001; Scribner *et al.* 2005; Holyoak *et al.* 2008; Nathan *et al.* 2008). However, dispersal is often difficult to observe directly. Landscape genetics and gene flow can offer insight into successful dispersal events, informing movement ecology theory (Nathan 2001) while offering guidance to conservation and management (Scribner *et al.* 2005).

Landscape genetics is a growing field that helps elucidate hierarchical, or multi-scale, population structure (Sunnucks 2000; Balkenhol *et al.* 2014), evolutionary history (Nathan 2001; Ficetola *et al.* 2007; Blair & Melnick 2012), disease ecology (Biek & Real 2010; Nobert *et al.* 2016), and landscape features that impact gene flow, or successful dispersal and exchange of genetics between populations, and movement (Nathan 2001; Adriaensen *et al.* 2003; McRae *et al.* 2008). Graph theoretic network models, where locations are connected between weighted line-segments, or edges, allow assessment of species' interactions with landscape features, and allow for identification of landscape barriers or resistances to species' movements. Using genetics to provide support for movement models focuses on understanding movements related to genetic exchange (Yannic *et al.* 2014), which provides insight into fragmented, yet connected, populations.

An initial step to understand gene flow in a metapopulation is to understand a species' current genetic composition on a landscape to determine if there are genetically distinct subpopulations. This requires consideration of temporal effects of potential barriers, and relative resistances of environment clines and gradients (e.g. precipitation gradients; Kershenbaum *et al.* 2014; Richardson *et al.* 2014). For example, Ficetola *et al.* (2007) found that the genetic

diversity and egg mortality in populations of the Italian agile frog (*Rana latastei*) was best explained by distance from glacial refugia combined with isolating effects of distance between populations. Similarly, Lugon-Moulin & Hausser (2002) found that genetic structure of a race of the common shrew (*Sorex araneus*) was influenced by distance from glacial refugia as well as contemporary barriers such as the Rhône River, with genetic signatures being ascribed to potential founder effects.

The interactions an animal has with habitat within its home range varies from how it interacts with habitat during dispersal (Clobert *et al.* 2009; Lookingbill *et al.* 2010; Centeno-Cuadros *et al.* 2011; Parks *et al.* 2013; Elliot *et al.* 2014; Pflüger & Balkenhol 2014; Peled *et al.* 2016). Expert opinion is often used to assign resistance costs, or quantified relative landscape hindrances to dispersal of an organism, to environmental parameters believed to influence movement (Spear *et al.* 2010).The use of expert opinion to parameterize resistance costs has been criticized for being too subjective (Spear *et al.* 2010; Sawyer *et al.* 2011; Shafer *et al.* 2012). While habitat modeling, Resource Selection Functions, or other habitat-use metrics offer more empirical methods (e.g. Shafer *et al.* 2012; Peterman *et al.* 2015), these models may miss important landscape features (Storfer *et al.* 2007) and may not adequately represent gene flow (Peterman *et al.* 2015).

Resistance costs are estimated either through least cost paths (LCP; Adriaensen *et al.* 2003), or isolation by resistance (IBR; McRae *et al.* 2008). LCP identifies a single, linear path between two points that minimizes the movement cost to an individual, whereas IBR incorporates multiple paths between two points. LCP and IBR offer two ends of the spectrum of hypothesizing how a species interacts with the environment during dispersal (Spear *et al.* 2010). A singular path may work for distinctly fragmented populations (Shafer *et al.* 2012; Trumbo *et*

al. 2013; Kershenbaum *et al.* 2014), but if populations exist along clines, it may not accurately represent connectivity and movement (Hamilton *et al.* 2006; Kershenbaum *et al.* 2014). Dispersing individuals may move across different paths to get between two locations; this has been demonstrated for wide ranging (McRae & Beier 2007), generalist (Munshi-South 2012), and even for some specialist species (Centeno-Cuadros *et al.* 2011; Peled *et al.* 2016). In these cases, IBR can increase robustness by incorporating more than one possible path (Alagador *et al.* 2012) and may perform better for gradient landscape features or clinal populations (Kershenbaum *et al.* 2014).

While relying on expert opinion to create resistance surfaces from landscape features is inherently subjective, these resistance surfaces can be supported and assessed empirically with correlation to genetic data (Zeller *et al.* 2012). Researchers have increasingly turned to using genetic distances as a proxy for rates of gene flow. Microsatellites are often used to identify distinct populations and estimate connectivity because they are neutral (no direct impact on fitness; Womble 1951; Epperson & Li 1997; Holderegger *et al.* 2006) and have a high mutation rate that allows for more rapid divergence from isolation (Balloux & Lugon-Moulin 2002). Unlike mitochondrial DNA (mtDNA), which can be applied to understand phylogeography and more historic events, microsatellites can offer insight into more recent movement and isolation (Wang 2010; Epps & Keyghobadi 2015).

With microsatellites, one can identify areas with unique genetic signatures through population clustering methods relying on Monte Carlo methods (Pritchard *et al.* 2000; Corander *et al.* 2003; Manel *et al.* 2005; Chen *et al.* 2007). However, for species where all populations are unknown or where populations do not exhibit uniform dispersion, pairwise genetic distances between individuals are informative and help account for inconsistent patch-based population

assignments (Coulon *et al.* 2006; Waples & Gaggiotti 2006; Jombart *et al.* 2008; Wasserman *et al.* 2010; Orozco-Ter-Wengel *et al.* 2011; Cushman *et al.* 2013). Barrier effects are identified by clustering individuals into populations, and then cline or environmental gradient costs can be identified using individual pairwise distances (Segelbacher *et al.* 2010), offering further insight into environmental resistance costs (Landguth *et al.* 2012).

Giant kangaroo rats (GKR; *Dipodomys ingens*) in the Ciervo-Panoche Natural Area (36°35'30" N, 120°40'30" W; CPNA) offer a unique opportunity to employ landscape genetics to understand how environmental factors impact gene flow of small mammals, which is poorly understood (Waits *et al.* 2016). GKR dispersing in the CPNA face a strong north-south precipitation gradient, topographic complexity, multiple vegetation communities, and roads. GKR dispersal events are difficult to detect, especially among juveniles. Previous work suggested that geographic distance did not explain genetic variation of GKR populations (Good *et al.* 1997; Loew *et al.* 2005; Blackhawk *et al.* 2016), indicating that landscape features may influence genetic composition and gene flow.

The underlying social structure and life history of GKR is critical for understanding dispersal. GKR are territorial, and individual burrow mounds are spaced approximately 10 meters apart, with neighbors of the opposite sex (Cooper & Randall 2007), often with neighbor-mate preference (Murdock & Randall 2001). During breeding, *Dipodomys* spp. increase mate-search distances around burrows without sex bias (Steinwald *et al.* 2013). *Dipodomys* spp., including GKR, are territorial against other small mammals (Hawbecker 1944; Frye 1983; Valone *et al.* 1995), and conspecific aggression has been noted in other *Dipodomys* spp. (Germano 2010). GKR and *Dipodomys* spp.do not have sex-biased dispersal distance (Skvarla *et al.* 2004; Edelman 2011; Blackhawk *et al.* 2016). Loew et al. (2005) estimated average GKR

dispersal events of females and males to be 99 and 120 meters respectively, but also noted one individual dispersed 700 meters using mark-recapture data.

Endemic to central California, GKR have a fairly limited distribution (Williams & Kilburn 1991; Figure 1), and were listed under the California Fish and Game Commission as state Endangered in 1980, and under the Federal Endangered Species Act in 1987 due to habitat loss (Williams & Kilburn 1991). Understanding how GKR dispersal is shaped by the landscape will ideally inform this species' conservation and management (Loew *et al.* 2005). Previous studies have suggested that the GKR in the CPNA may be structured into three or more sub-populations located in the Panoche Valley, Tumey Hills, and Ciervo Hills (Loew et al. 2005; Figure 2) with evidence that patchy distribution of GKR in the northern range has persisted prior to anthropogenic-caused range contractions (Grinnell 1932). There is likely very low individual natal and mating dispersal, and the CPNA has previously been identified as having at least 3 subpopulations from mtDNA, representing a more historic population structure (Good *et al.* 1997). The Panoche Valley population is likely the oldest in the area, and is likely a centroid for genetic diffusion across patches, while the Tumey Hills population and Ciervo Hills population are more recent (Good *et al.* 1997).

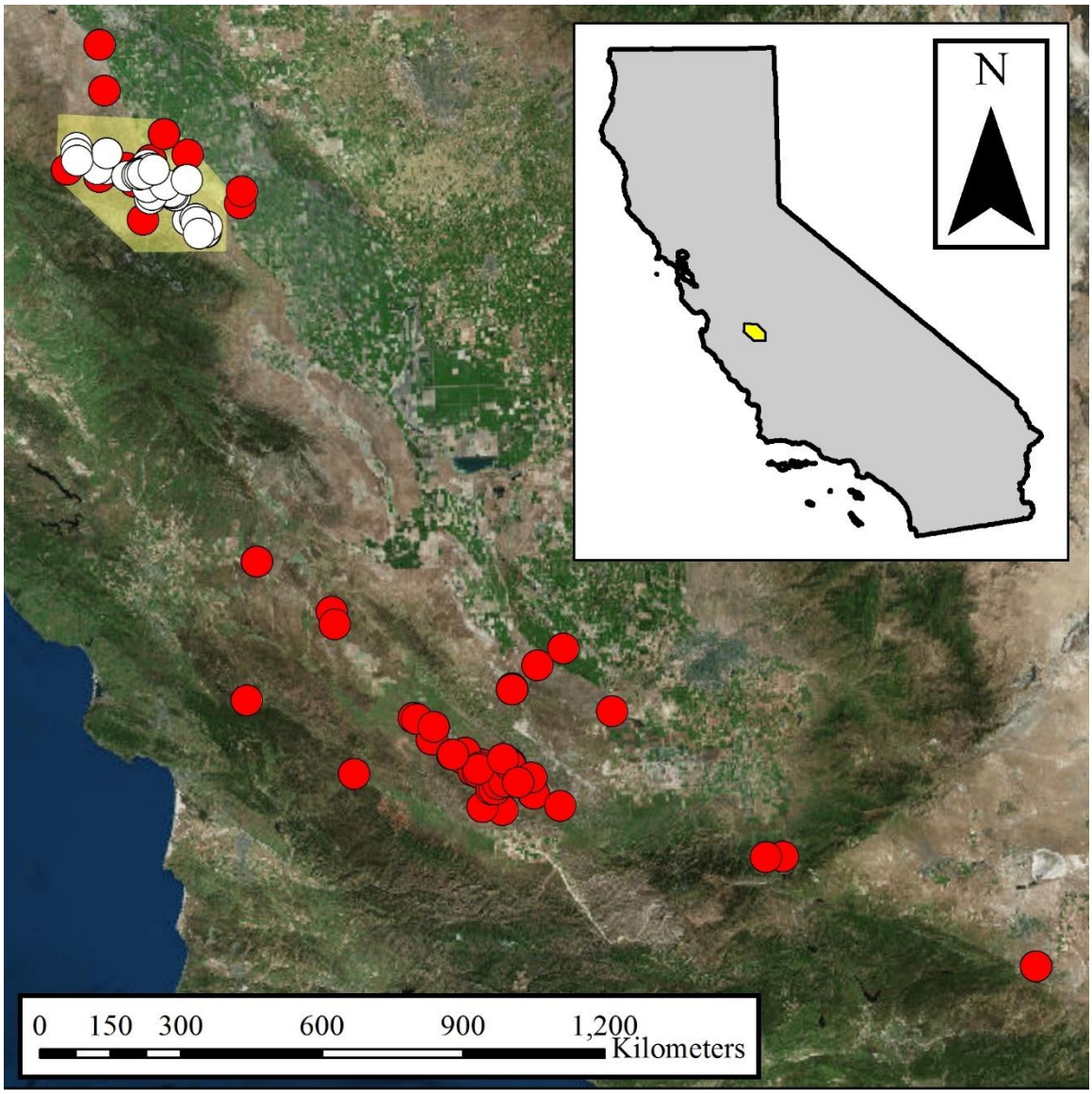

Figure 1: Geo-referenced occurrences of GKR from the Global Biodiversity Index Database (red circles, n=210; GBIF 2016), and 2013 and 2014 trapping data confirmed GKR from genetic analysis (white circles, n=121). The study area of the CPNA is depicted in yellow.

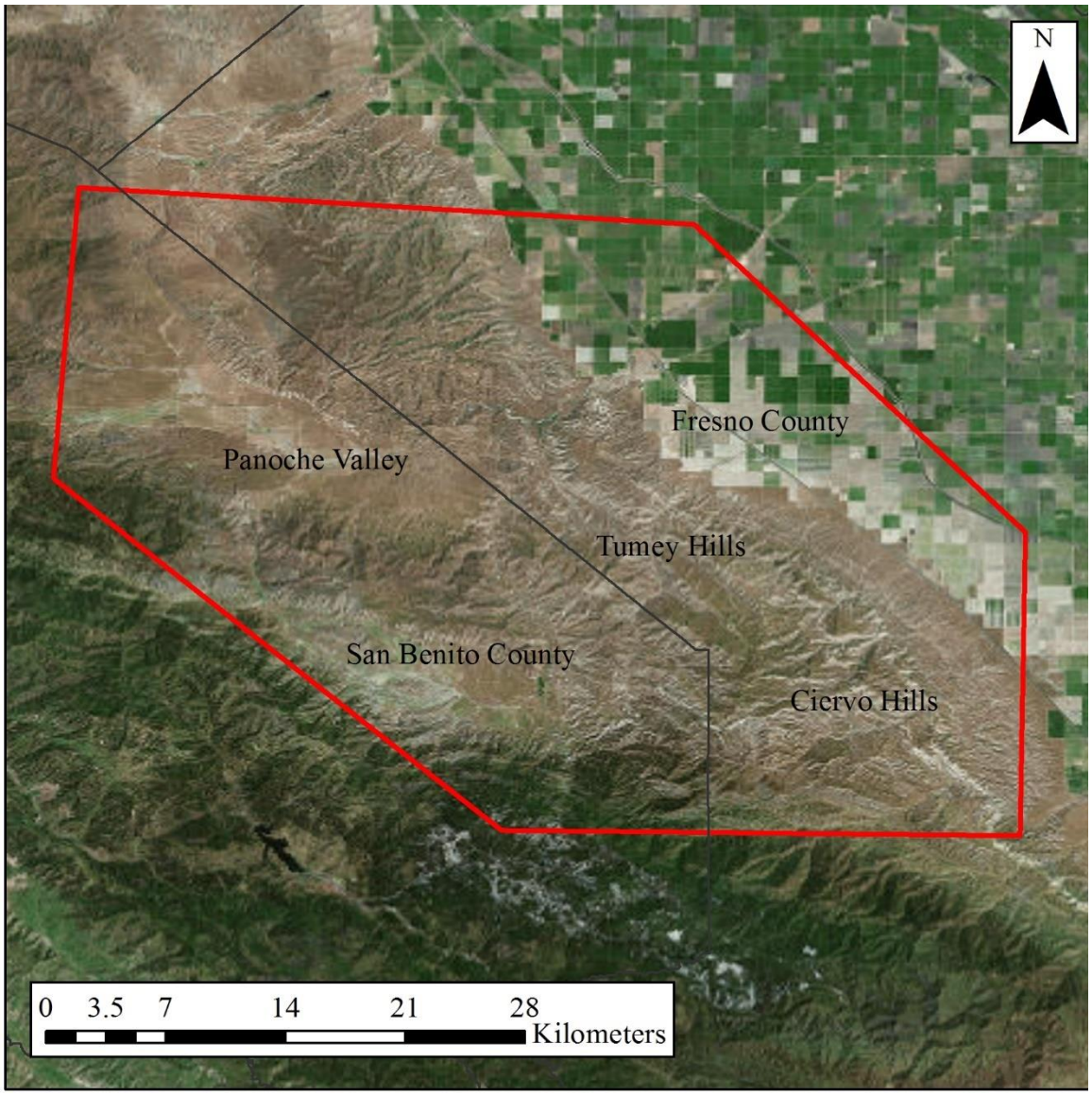

Figure 2: Locations of Panoche Valley, Tumey Hills, and the Ciervo Hills within the study area (red).

I identified four parameters as potential influences on GKR dispersal from existing literature and the landscape features of the CPNA: precipitation, slope, vegetation, and roads. The CPNA is a topographically complex landscape with a strong north-south moisture and precipitation gradient (Bean *et al.* 2014a), which is a driving factor in GKR habitat suitability (Bean 2012). While areas with slope less than 10 degrees have been identified as being important

for GKR habitat (Grinnell 1932; Shaw 1934; Bean *et al.* 2014b), slope is also a tangible dispersal cost, and may influence gene flow and individual movement due to direct energetic costs.

Historically, the CPNA was dominated by native bunch grasses (Grinnell 1932; Shaw 1934; Hawbecker 1944), but these have been replaced by invasive annual grasses, primarily red brome (*Bromus madritensis rubens*; Germano *et al.* 2001, 2011) which may impact movement by creating more dense groundcover (Germano *et al.* 2001). Native annual grasses are an important predictor of GKR presence (Bean *et al.* 2014b), and GKR may select pathways that have food resources or exhibit natal-preference dispersal.

Roads provide an interesting parameter for GKR dispersal. GKR burrows have been found in berms 2m from roads, but not in compacted soils (Harris *et al.* 1987). Brock & Kelt (2004) found that there was higher individual turnover for Stephen's kangaroo rats (*Dipodomys stephensi*) along dirt roads, possibly indicating migrating individuals use roads as dispersal corridors, or that roads are population sinks with higher mortality and individual replacement. There are also two creeks, Panoche Creek and Silver Creek, which may act as corridors and aid in GKR dispersal (Loew *et al.* 2005), or act as a barrier if GKR cannot cross these creeks easily during dispersal events (Good *et al.* 1997).

In this study, I describe the impacts of landscape parameters on GKR genetic structure and gene flow while comparing techniques often used in landscape genetic analyses. First, I assessed genetic-spatial clustering of GKR populations in the CPNA and assessed genetic variance between the proposed populations to determine if genetically unique populations were identifiable and could help define barriers between GKR populations. Second, I identified genetic structure of individuals across the landscape. Third, I identified related individuals and calculated straight-line geographic distance between them to determine dispersal. Fourth, I

assessed the correlation between hypothesized cost maps (IBR and LCP) and individual genetic distances (proportion of shared alleles, codominant marker distance) to determine landscape features that influence gene flow. Fifth, I assessed which model, LCP or IBR, best explained GKR genetic variation. I predicted that there would be 3 populations identified from clustering methods that coincided with previously identified populations, that there would be high genetic variation of individuals across the landscape, and that there would be low to no dispersal distance between related individuals. I predicted that non-grassland vegetation, high slope, absence of roads, and high precipitation negatively impact GKR connectivity. I predicted that GKR movement would be diffuse due to multiple paths being passable for GKR, meaning that IBR would better describe GKR gene flow than LCP.

Methods

Field researchers target trapped at GKR burrow entrances in a continuous sampling design across the CPNA from 2013-2015, collecting hair samples for genetic analyses. We used extra-long Sherman live traps baited with millet (Valone *et al.* 1995; Thibault *et al.* 2010), focusing mostly along roads due to accessibility. We set between 4 and 61 traps per site, with trap sites at least 100 m apart (Bean *et al.* 2014b). Traps were opened at 18:00-21:00 (after sunset) and checked at 3 hour intervals. Traps were closed after midnight. Each site was trapped for 3-5 days (Bean *et al.* 2014b). Each kangaroo rat was ear tagged and hair follicles were collected in accordance with U.C. Davis protocols for genetic analysis (T. Bean pers. comm. 2014, L. Hernandez pers. comm. 2015). Two hair samples were collected from each back haunch of a kangaroo rat using latex gloves and tweezers. The hair was then placed in a centrifuge tube filled with a 95% alcohol solution. Between individuals, the tweezers were sterilized with a 10%

bleach solution and then rinsed with water or an isopropyl wipe. U.C. Davis performed microsatellite amplification and identification for 15 loci for the 2013 and 2014 genetic samples. I collected 34 geo-referenced GKR genetic samples from 2014 to complement the 87 samples obtained in 2013 (Bean *et al. unpublished data*), leading to a total sample size of 121 geo-referenced individuals and a total of 123 individuals with genetic data (2 individuals had genetic data but were not geo-referenced; Figure 3).

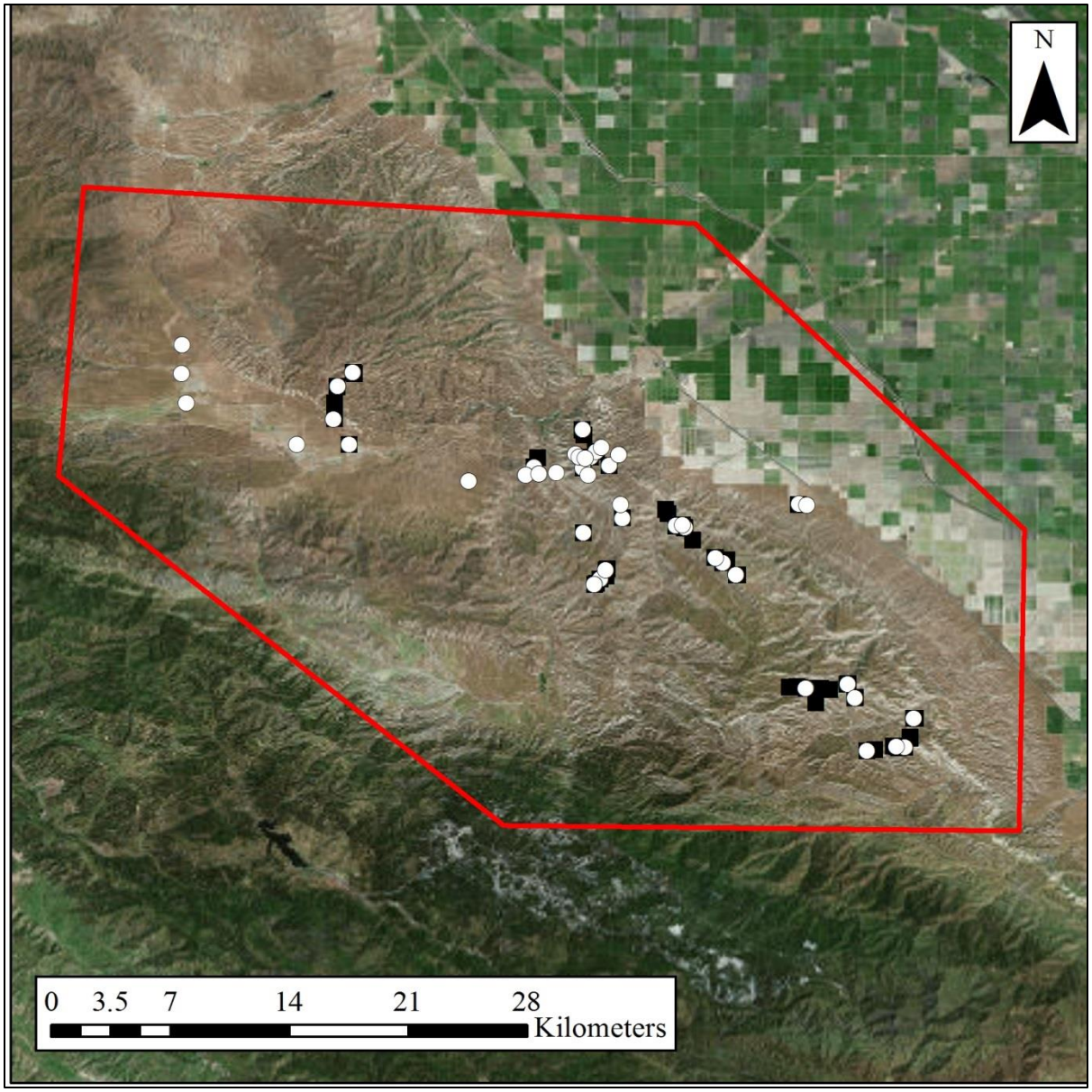

Figure 3: Genetic sample locations of GKR (n=121) from 2014 (white circles) and 2013 (black squares)

Hardy-Weinberg Proportions

Hardy-Weinberg Proportion (HWP) and Linkage Disequilibrium (LD) were evaluated using exact tests with 20 batches of 10,000 iterations and a dememorization of 10,000 in

GENEPOP 4.2 (HWE; Raymond & Rousset 1995; Rousset 2008) with p-values adjusted for multiple testing using a false discovery rate (Benjamini & Hochberg 1995) of alpha= .05. LD was evaluated by randomly assorting individuals into 2 populations (A and B). If LD was identified for both populations A and B, then the paired loci would be assumed to be linked, and would be removed. if LD was identified in either population A or B but not the other, the paired loci would be assumed to not be linked and that the apparent linkage would be considered due to sampling and population structure (Waples 2015, L. Hall pers. comm. 2016).

Assuming a single population for GKR, 6 Loci (dst1318, dst1567, dst2887, dst3158, dst3268, and dst3646) significantly deviated from HWP using the adjusted p-values due to a deficiency in heterozygosity. To determine if this was a Wahlund effect (Wahlund 1928), where loci were not in proportion due to fixation in subpopulations, or null alleles, where HWP violation is due to failure to amplify all alleles, HWP heterozygosity between all individuals and within the populations identified by TESS (see Population Structure methods and Population Structure results) was calculated. Locus dst1318 appeared to be heterozygous-deficient for all three populations and was removed due to null alleles (Waples 2015, Hall pers. comm. 2016). Even when dividing individuals based on population, Population 2 had a remarkable number of heterozygous deficient loci (dst2887, dst3268, and dst3646 deviated from HWP at p-value < .0001 after dst1318 was removed) even though it had the largest sample size (n=82). To determine if this was a response of hierarchical genetic structure, TESS was re-run only including population 2. However, based on individual assignment probabilities (Figure 4), splitting this subpopulation into two subpopulations was not accepted. The remaining 5 loci that significantly deviated from HWP were most likely due to violating HWP's assumption of large population size and migration, and the failure of population clustering programs to identify

genetic subgroups. None of the loci were in linkage disequilibrium and 14 loci were kept in the individual pairwise analyses.

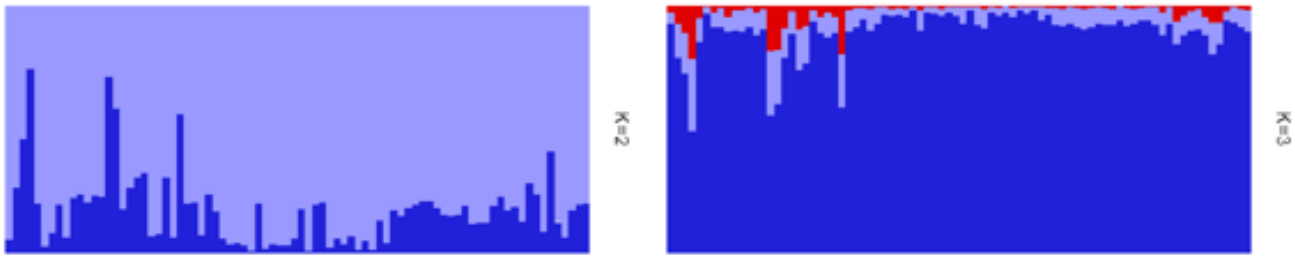

Figure 4: Individual cluster assignment from TESS of GKR within population 2 arranged from West to East (K=2: simulations=100, permutations=1,000,000 burn in=100,000, K=3: simulations=58, permutations=1,000,000 burn in=100,000) under the CA

Population Structure

I used individual genetic samples to assess GKR population structure within the CPNA. I relied on two common approaches to describe population genetic structure, TESS (Chen *et al.* 2007) and STRUCTURE (Pritchard *et al.* 2000; Falush *et al.* 2003; Hubisz *et al.* 2009). Program TESS, which predicts spatial Bayesian clustering through tessellations and Markov Chain Monte Carlo, is a promising alternative to STRUCTURE. The main difference between STRUCTURE and TESS is that STRUCTURE minimizes divergence from Hardy-Weinberg Proportions and Linkage Disequilibrium while TESS highlights genetic-spatial auto-correlation ((François & Durand 2010). TESS incorporates geospatial referencing (Chen *et al.* 2007), and can better describe clustering of individuals with limited movement (Coulon *et al.* 2006). This makes it a potentially better approach for GKR population delineation. TESS has low mis-assignments, can handle migrants, and is good at detecting a recent contact zone and/or weak genetic differentiation under the assumptions of populations overlapping between 2 to 30%, although uneven sampling across a genetic cline creates difficulty in identifying true population

boundaries (Chen *et al.* 2007). STRUCTURE can identify unique populations better than TESS when population boundary overlap is 40%, and did better at identifying boundaries along allele frequency clines (Chen *et al.* 2007). Although STRUCTURE may not perform as well given the trapping methodology (Chen *et al.* 2007; Hubisz *et al.* 2009), it is a common method in the literature. I used all 15 loci to identify genetic clusters, all 123 individuals for STRUCTURE, and the 121 georeferenced individuals for TESS.

For TESS, neighborhood trees and Voronoi cells were created for the geo-referenced 121 individuals, and a codominant admixture (CAR) model was run, clustering individuals into 2 through 7 populations (K) using geographic location as a prior (n=100 simulations/cluster, permutation=1,000,000, burn in=100,000). Admixture models increase robustness in identifying genetic fusion and fission processes (François & Durand 2010), and are more common in nature (Jay *et al.* 2011). One hundred seventy simulations were run for K=2 at the same settings instead of 100 due to a computer restarting mid-run and the code being executed again. The simulations were merged for each K using the R package *pophelper* (Francis 2016) and CLUMPP version 1.1.2 (Jakobsson & Rosenberg 2007). The number of subpopulations (K) was inferred based on individual assignment probability plots.

For STRUCTURE, the full sample (n=123) was run with no location-informed prior. Between 2 and 7 populations (K) were analyzed (n=100 simulations/K, permutation=100,000, burn in=1000) with a CAR model. Selected number of clusters was determined by the Δ K Method (Evanno *et al.* 2005). The 100 simulations/K were merged and the Δ K Method (Evanno *et al.* 2005) was conducted using the R package *pophelper* (Francis 2016). STRUCTURE was also run with only the 121 individuals used in the TESS analysis to determine if omitting 2 GKR would bias the results.

To better understand how individual genetics were arranged spatially, I estimated genetic distances using proportion of shared alleles (Dps; Bowcock *et al.* 1994; Galpern *et al.* 2014) to create a Moran Eigenvector Map (MEM) using the R package *memgene* (Galpern *et al.* 2014), and looked at spatial autocorrelation for Dps and codominant marker distance (GenAlEx; Smouse & Peakall 1999; Peakall & Smouse 2006, 2012). Genetic MEMs allow visual display of cryptic genetic neighborhoods (Galpern *et al.* 2014) while accounting for space and produce genetic eigenvalues from genetic distance matrices that are not auto-correlated (Borcard & Legendre 2002). Dps often represents more fine scale genetic structure and can elucidate genetic variation between individuals (Laurence *et al.* 2013), increasing the amount of variation displayed by the MEM.

Dispersal

I identified all full- and half-siblings and measured the straight-line geographic distance between their capture locations to assess dispersal distances between related individuals. I used COLONY v. 2.0.6.1 (Jones & Wang 2010; Wang 2012, 2016), a Bayesian model that optimizes maximum likelihood for full- and half-sibling assignment simultaneously (Wang 2004; Jones & Wang 2010), to infer full- and half-sibling pairs. All individuals were simultaneously considered potential offspring and potential parents. Potential fathers consisted of the known males (n=60) and unknown sex (n=7), and potential mothers consisted the known females (n=52) and unknown sex, with all loci assumed to not have null alleles from HWP testing (n=14) included for parentage analyses.

Polygamy was assumed for both males and females with the potential for inbreeding. No prior was used, and the probability of having a father or mother parent in the dataset was set to 0.5 with genotyping error probability set to .02 (e.g. Wang 2004 turtle dataset). COLONY is robust to marker error rates, but marker error rates are necessary for the parameter searching algorithms, or else spurious sibling inferences are made (Wang 2004). Allele frequencies were scaled by sib-ship with 3 “Long” runs set to “High” likelihood. Allele frequencies and sib-ship scaling were set to update during the model runs. Siblings and half-siblings were considered true if the mean probability minus one standard deviation was above .9 and .95, respectively, calculated from ten COLONY outputs.

Connectivity Modeling

I generated a series of connectivity models and determined their correlation to genetic distance matrices using Dps and codominant marker distance. I created resistance surfaces, rasters of quantitative costs of parameters, incorporating: slope (U. S. Geological Survey 2014),

mean annual precipitation (U. S. Geological Survey 2006), vegetation type (U.S. Forest Service 2010), and roads (U. S. Census Bureau 2008a; b).

Increasing the difference between parameter costs in resistance surfaces offers more insight into landscape-genetic associations, and influences model selection (Koen *et al.* 2012). In order to verify models were parameterized correctly, I created alternative hypotheses on how cost assignment of each parameter could impact GKR dispersal including:

Precip Linear: Cost increases as annual precipitation increases

$$Cost = \frac{Precipitation}{maximum(precipitation)} * 1000$$

Precip Thresh 300: Cost is a threshold at 300 mm of annual precipitation (less than cost=1, equal to or more than cost=1000)

Precip Thresh 250-350: There is an optimum precipitation range between 250 and 350 mm (cost between 250 and 350 mm=1, less than or more than cost=1000)

Slope Linear: Cost continuously increases as slope increases

$$Cost = \frac{Slope}{maximum(Slope)} * 1000$$

Slope Thresh 5: Cost is a threshold at 5 degrees (less than=1, more than=1000)

Slope Thresh 10: Cost is a threshold at 10 degrees (less than=1, more than=1000)

Veg Multi: Vegetation type has varying levels of costs (see Appendix A for classification)

Veg Binary: Grass, pastures, and barren areas have essentially no resistance (cost=1) while all other habitat types are costly (cost=1000)

Road Conductance: Roads facilitate movement (road cost=1, non-road cost=1000)

Road Resistance: Roads hinder movement (road cost=1000, non-road cost=1)

For additive models, categorical variables were assigned a resistance cost based on available literature (Appendix A), and then each hypothesized cost map was constrained (divided by the maximum cell value). The constrained value can offer a way to compare between models effectively (Trumbo *et al.* 2013; Kershenbaum *et al.* 2014) because cost distances are relative to the maximum landscape variance of the parameter (Legendre *et al.* 2015, see Mateo-Sánchez *et al.* 2015).

Raster resolution was set to approximately 28 square meters based on the minimum freely available data cell size. The precipitation raster was originally 800 square meters, but was

resampled to the resolution of the other parameters using nearest-neighbor in the "resample" command from the package *raster* version 2.5-2 in R (Hijmans 2015). To test the sensitivity of parameter selection, I created multiple models of precipitation, slope, vegetation, and roads based on power functions (e.g. Epps *et al.* 2013) ranging between 0-2, increasing by .5 per trial. Because movement costs may not be linear, I modeled exponential impacts of landscape effects by 100^(Cost surface) and 100-100^(1-Cost surface; Trumbo *et al.* 2013). I calculated cost surfaces based on the full model:

Full: Gene flow ~ Precipitation + Slope + Vegetation + Road

Working under the null models of Isolation by Distance:

IBR: Gene flow ~ Standardized Cost Surface (cost=50, e.g. Zeller et al. 2016)
LCP: Gene flow ~ Straight-Line Geographic Distance

I also employed a more empirical method assigning quantitative costs to a resistance surface using the niche-modeling program, MaxEnt (Phillips *et al.* 2006). Creating a cost surface from a habitat model offers an empirical method for determining cost values that resolves some of the criticisms of using expert driven models (Wang *et al.* 2008; Spear *et al.* 2010), as well as patch cohesion possibly influencing connectivity (Cushman *et al.* 2012). Using the vegetation, road, precipitation, and slope parameters in iterative combinations, a MaxEnt model was generated using GKR site occurrences from 2011-2015 trapping in the CPNA (n=99 unique presence locations). Smoothing parameters (betas) ranging from 1 to 4 were evaluated with the models as well. Model selection was executed using Akiake's Information Criterion corrected for small sample size (Burnham & Anderson 2002) in ENMTools (Warren *et al.* 2010; Warren & Seifert 2011). The MaxEnt model selected for all variables with 26 parameters and a smoothing coefficient of 1 (Δ AICc = 68.76 to next model, Appendix B). The MaxEnt habitat suitability model was analyzed as a "conductance" (1/resistance), inverting the MaxEnt raster in the

resistance raster generation, and as a resistance, where the MaxEnt habitat suitability was assumed to equate to resistance, in Circuitscape (McRae *et al.* 2013) because suitable habitat may be easy to move through (see Schwartz *et al.* 2009; Shafer *et al.* 2012), or these areas may not be viable dispersal routes due to territoriality of local animals, or the dispersers may settle in these areas, limiting the rate of gene flow.

Next, I compared these connectivity models to individual genetic distances. I conducted pairwise correlation analyses between IBR cost distances and individual genetic distances through partial mantel tests (Smouse *et al.* 1986) with bootstrapping without replacement (1,000,000 permutations, 1000 bootstrap; e.g. (Kershenbaum *et al.* 2014) using the mantel function from the R-package *ecodist* (Goslee & Urban 2007). Partial mantel tests account for the influence of geographic distance while estimating the correlation between genetic and environmental dispersal cost distance. A mantel test (Mantel 1967) with genetic distance and the null models were included (Jenkins *et al.* 2010). All pairwise connections were considered in the models because full networks are more robust (Naujokaitis-Lewis *et al.* 2013).

To ensure that the cost surface accurately explains the genetic distance without spurious correlations, I employed causal modeling (Wang & Summers 2010; Cushman *et al.* 2013) to determine if cost surfaces would explain genetic variance while accounting for other hypothesized resistances. Causal modeling relies on partial mantel tests where, instead of geographic distance being accounted for, another statistically significant model is used. If a model is still statistically significant after accounting for the other hypothesized costs, it is accepted. Causal modeling and partial mantel tests have the advantage that there is little effect of number of individuals sampled on the magnitude of the Pearson's correlation, although the predictive power increases (Landguth *et al.* 2012; Zeller *et al.* 2016).

To ensure that sampling extent did not mask fine-scale genetic structure, I calculated cost surface distances between individuals within 3km from each other (Row *et al.* 2010; Keller *et al.* 2013; van Strien *et al.* 2015). Three km was used because genetic distances were more highly correlated within 3km than expected at random using GenAlEx (3km; Peakall & Smouse 2006, 2012; Banks & Peakall 2012). Because genetic variation becomes constant and is not influenced by immediate dispersal, cost surfaces and isolation by distance can be masked due to sampling extent.

Results

Population Structure

STRUCTURE identified four populations from the Δ K Method (n_1=34, n_2=20, n_3=19, n_4=39, with 11 individuals that were assigned a high level of admixture and no discernable population of origin; Figure 5-7), and TESS identified three populations (n_1=22, n_2=82, and n_3=17; Figure8-9) from visual display of population assignment probabilities. Both STRUCTURE and TESS had low Fst values between the identified populations (

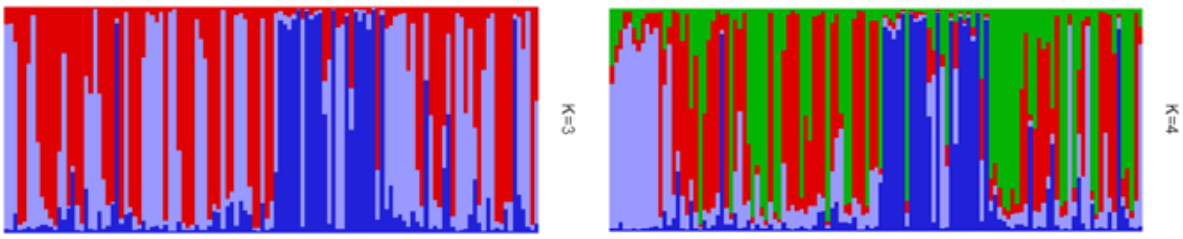

Figure 11: Individual cluster assignment of geo-referenced GKR (n=121) arranged from West to East (simulations/K=100, permutations=100,000, burn in=1,000) under the CAR admixture model. Number of Clusters was inferred from the Δ K Method to K=3.

559

Table 1-2), and high credible intervals around individual assignment probabilities (Appendix C), and a high level of admixture. When the two additional individuals were omitted from STRUCTURE, STRUCTURE identified only 3 populations through the Δ K Method (Figure 10), with a high level of admixture in the eastern population (Figure 11).

TESS did not identify the Panoche Hills population that STRUCTURE did. STRUCTURE is more likely to identify family groups when full-siblings are included, but is relatively robust to the inclusion of half-siblings (Anderson & Dunham 2008). When full-siblings (n=4) and half-siblings assigned with a greater than 95% probability (n=10) were removed, and re-analyzed (n=109) in STRUCTURE and TESS, STRUCTURE still identified 4 populations using the Δ K Method, but TESS clustered individuals into one population based on visual display of individuals' assignment probabilities. Mean allelic richness for identified populations ranged between 8.29 and 12.79 for STRUCTURE and 9.57 and 13.5 for TESS (Appendix D)

Genetic distances between individuals were not auto-correlated to straight-line geographic distance, but they were correlated at ranges less than 3km for both Dps (Figure 12) and codominant marker distance (Figure 13). The MEM depicts the spatial correlation of genetic structure (Figure 14), with the first principle component of the individual genetic distance ranging between -.15 and .15.

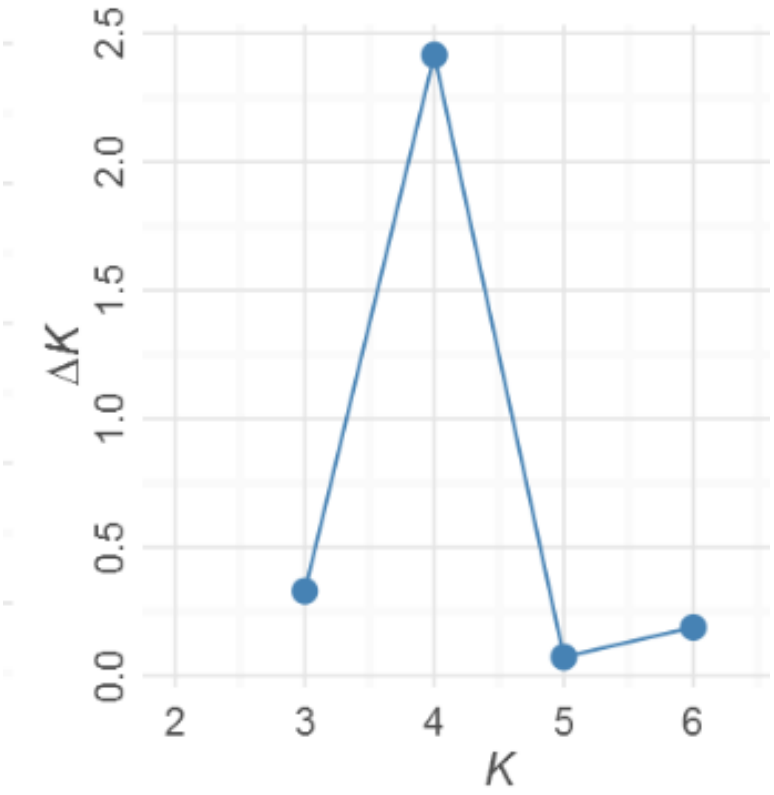

580

581 **Figure 5:** From observing the delta K, we see that 4 clusters optimize the change in Log
582 Likelihood according to the Δ K Method.

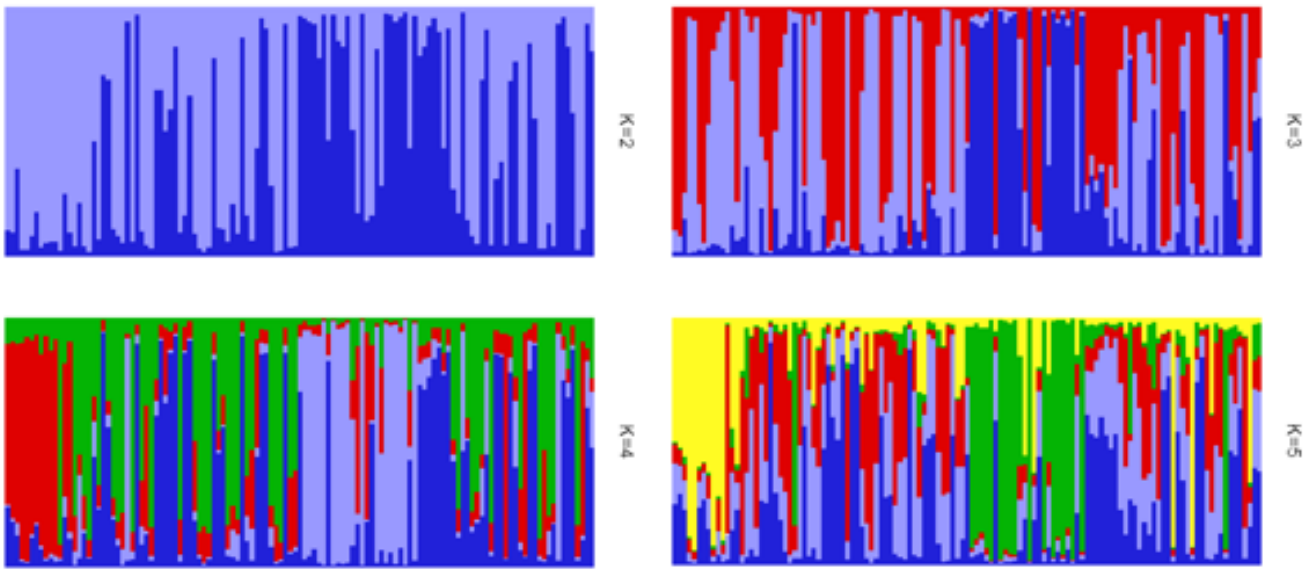

583

584 **Figure 6:** Individual cluster assignment of GKR (n=123) arranged from West to East
585 (simulations/K=100, permutations=100,000, burn in=1,000) under the CAR admixture
586 model. Number of Clusters was inferred from the Δ K Method to K=4.

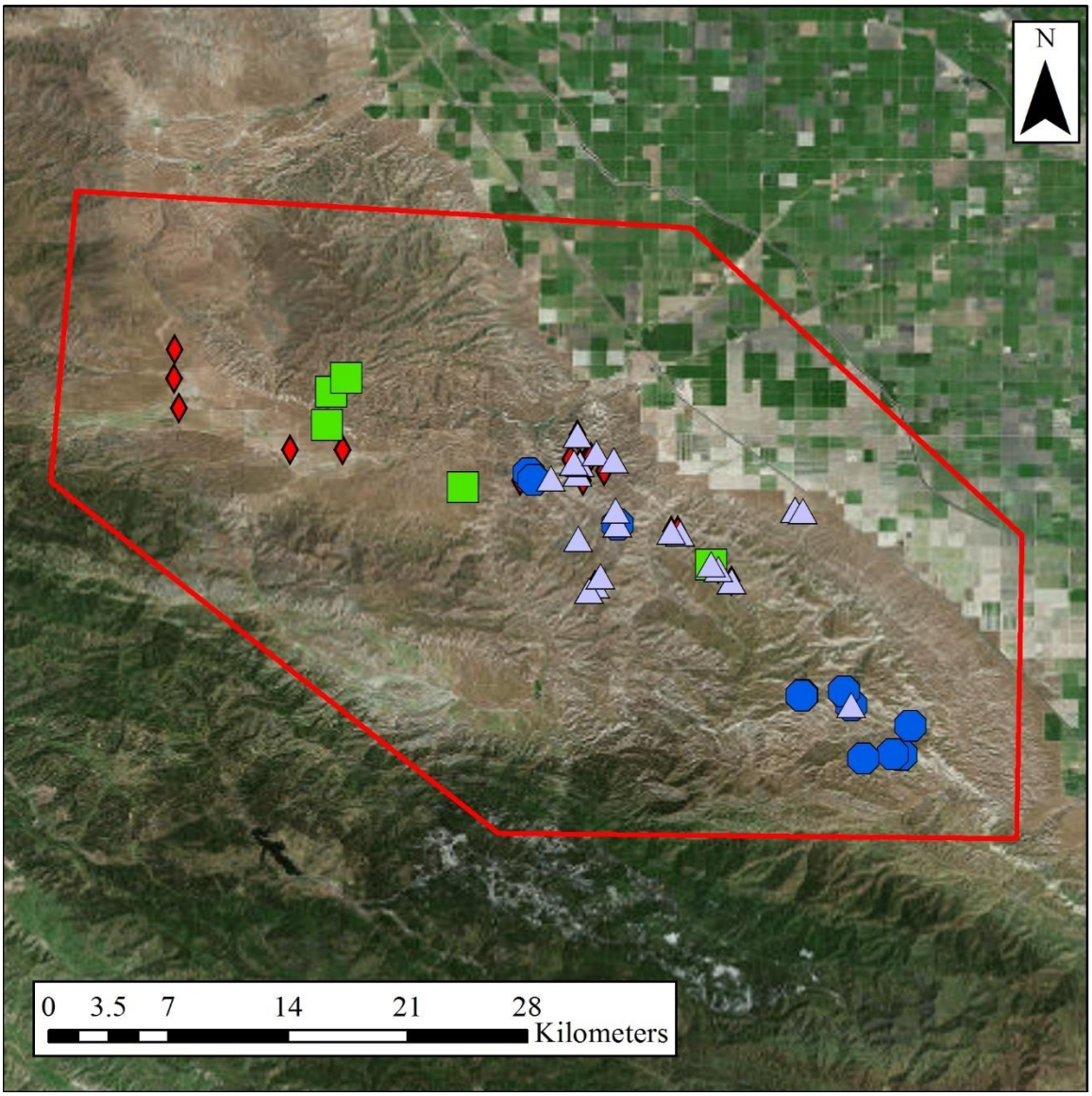

587

588 **Figure 7:** The population assignments for Panoche Valley (red diamonds), Panoche Hills (green
589 squares), Tumey Hills (purple triangles), and Ciervo Hills (blue circles) from
590 STRUCTURE.

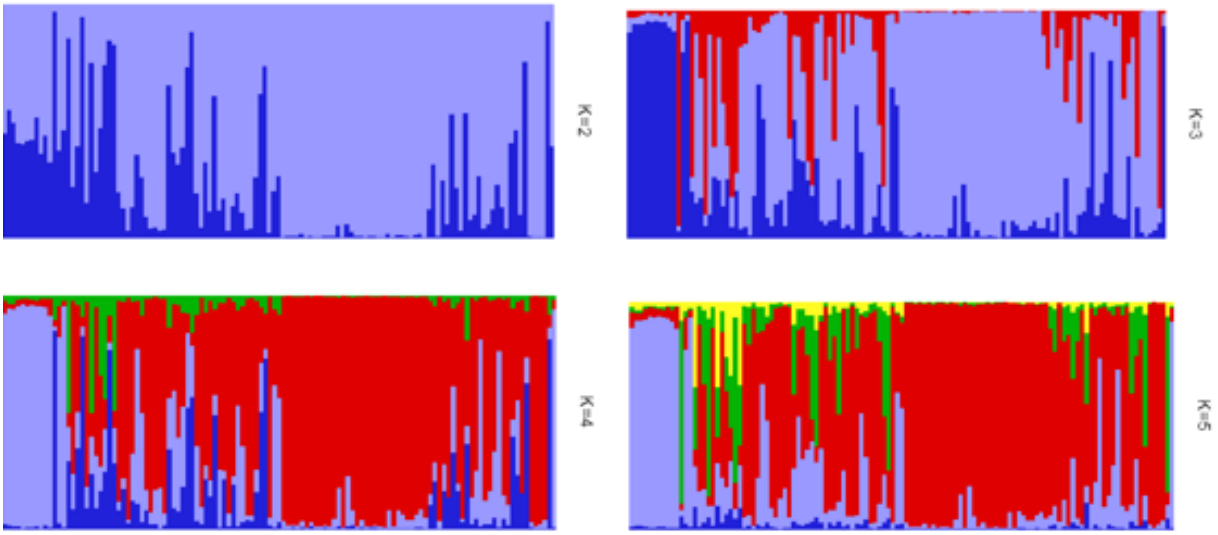

Figure 8: individual cluster assignment from TESS of GKR (n=121) arranged from West to East (simulations/K=100, permutations=1,000,000 burn in=100,000) under the CAR admixture model. Given the high assignment probabilities for individuals for K=3

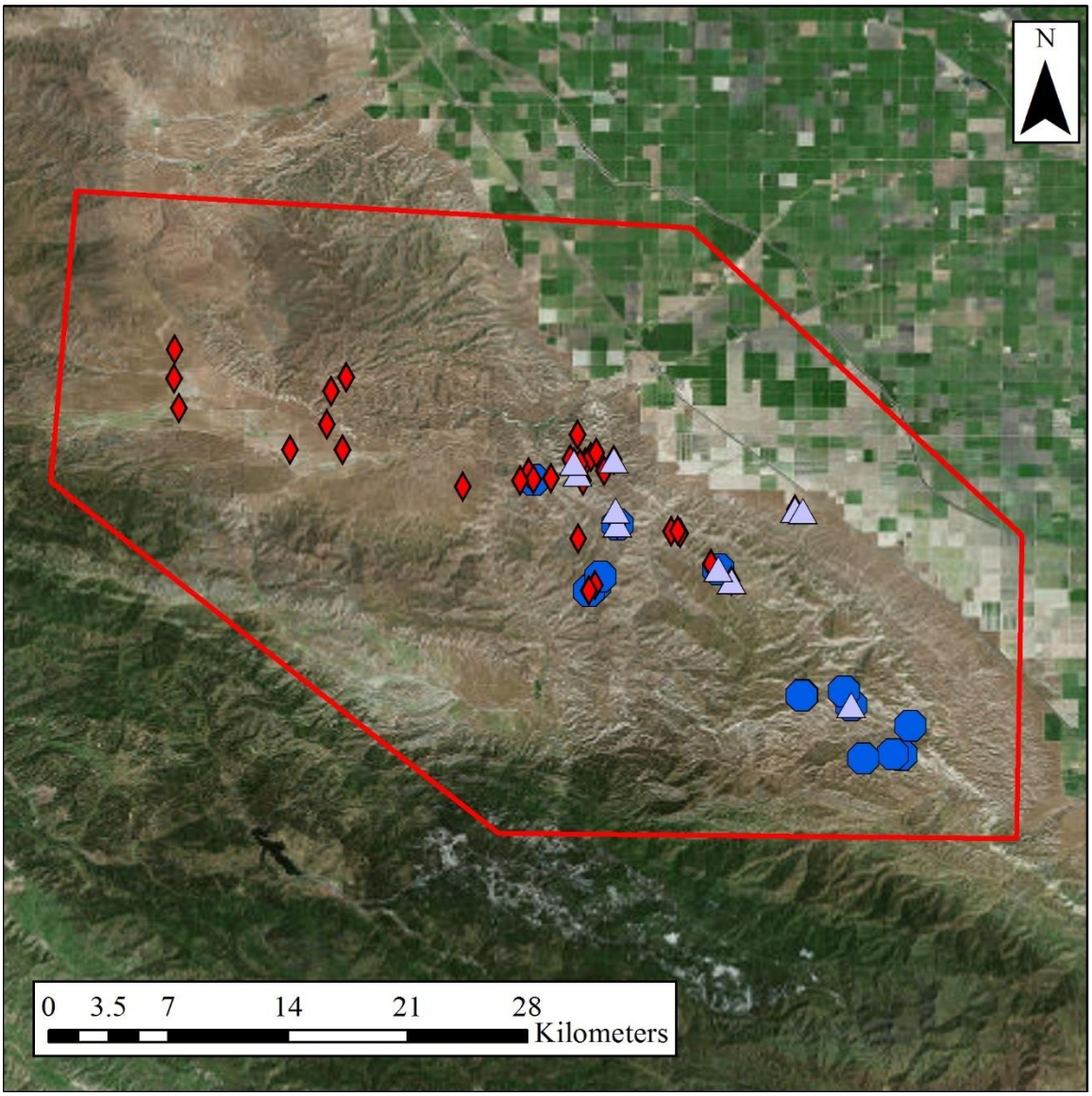

595

596 **Figure 9:** The population assignments for Panoche Valley (red diamonds), Tumey Hills (purple
597 triangles), and Ciervo Hills (blue circles) from TESS.

598

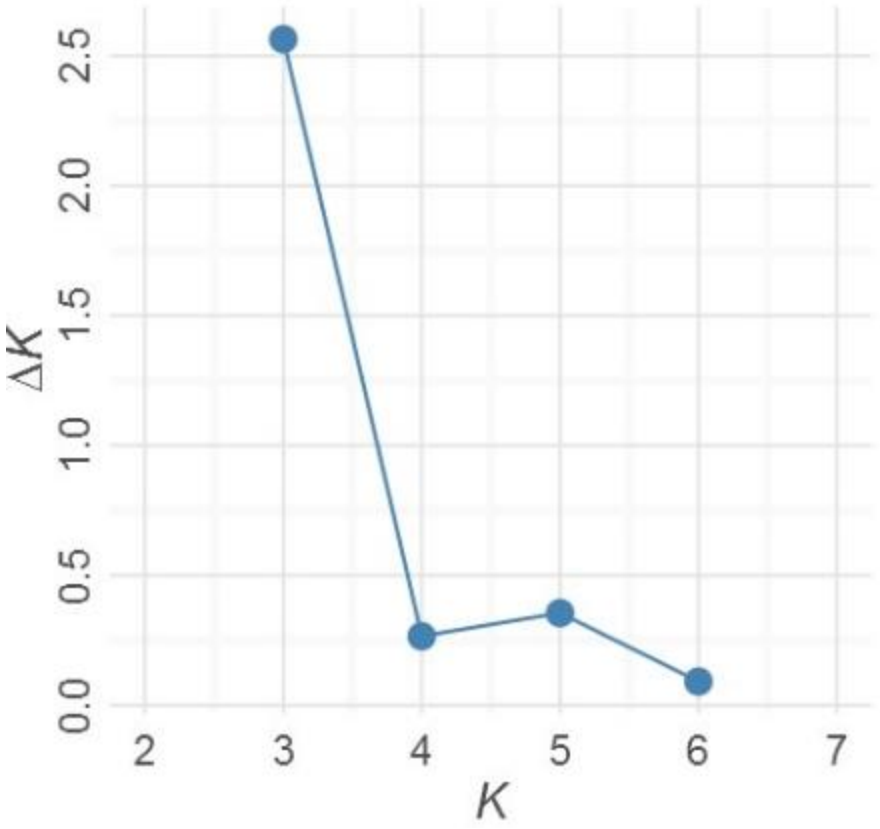

599

600 **Figure 10:** From observing the delta K omitting the 2 non-georeferenced GKR, we see that 3
601 clusters optimize the change in Log Likelihood according to the Δ K Method.

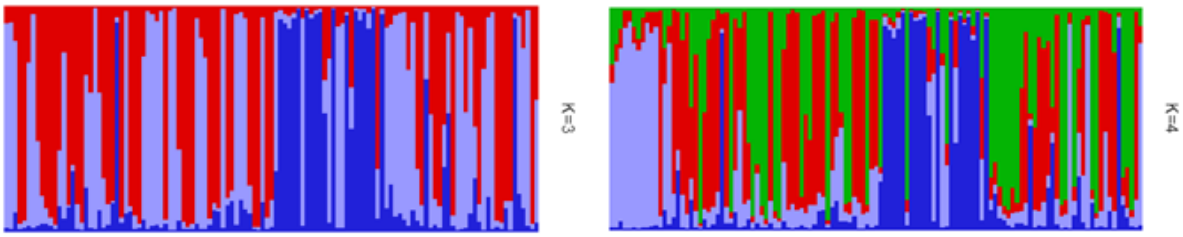

602

603 **Figure 11:** Individual cluster assignment of geo-referenced GKR (n=121) arranged from West to
604 East (simulations/K=100, permutations=100,000, burn in=1,000) under the CAR
605 admixture model. Number of Clusters was inferred from the Δ K Method to K=3.

606

607

608

609

610 **Table 1:** Fst values between the 3 identified populations from TESS. Fst values were calculated
611 in GenAlEx (excluding locus dst1318, permutations=9999, bootstrap=999; Peakall &
612 Smouse 2006, 2012).

Population A	Population B	Fst	P-value
Ciervo Hills	Panoche Valley	0.024	0.001
Ciervo Hills	Tumey Hills	0.036	0.001
Panoche Valley	Tumey Hills	0.029	0.001

613

614

615 **Table 2:** Fst values between the 4 identified populations from STRUCTURE. Fst values were
616 calculated in GenAlEx (excluding locus dst1318, permutations=9999, bootstrap=999;
617 Peakall & Smouse 2006, 2012).

Population A	Population B	Fst	P-value
Panoche Valley	Panoche Hills	0.030	0.001
Panoche Valley	Tumey Hills	0.032	0.001
Panoche Hills	Tumey Hills	0.042	0.001
Panoche Valley	Ciervo Hills	0.020	0.001
Panoche Hills	Ciervo Hills	0.027	0.001
Tumey Hills	Ciervo Hills	0.029	0.001

618

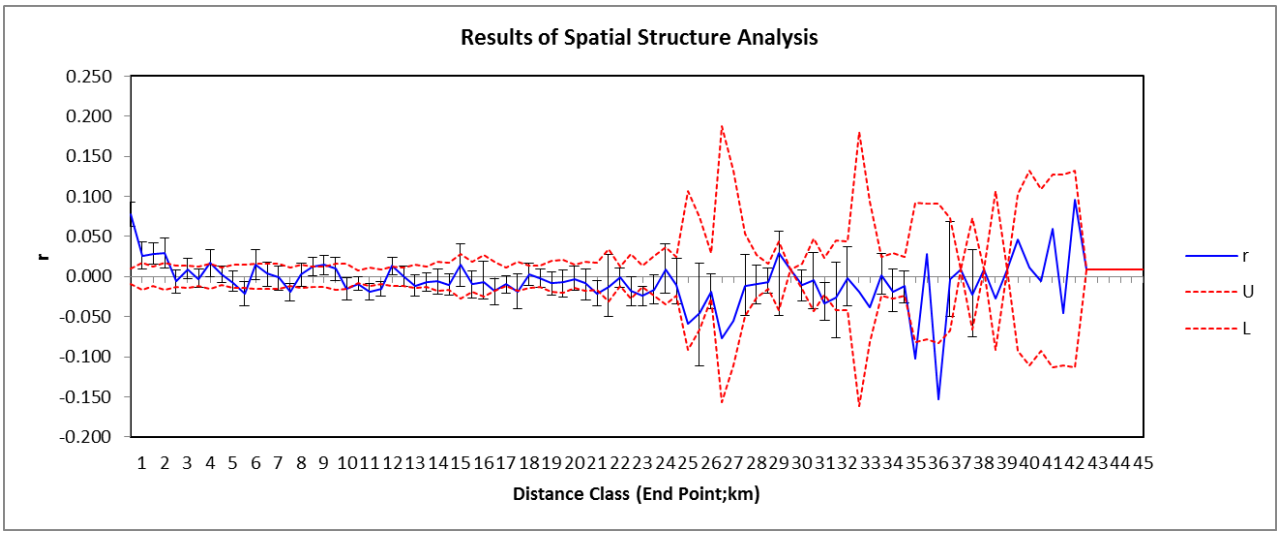

Figure 12: Individual Dps distance based on 14 loci is not autocorrelated to straight-line geographic distance at greater than 3km, however there is slight autocorrelation at less than 3 km (GenAlEx; Peakall & Smouse 2006, 2012; Banks & Peakall 2012).

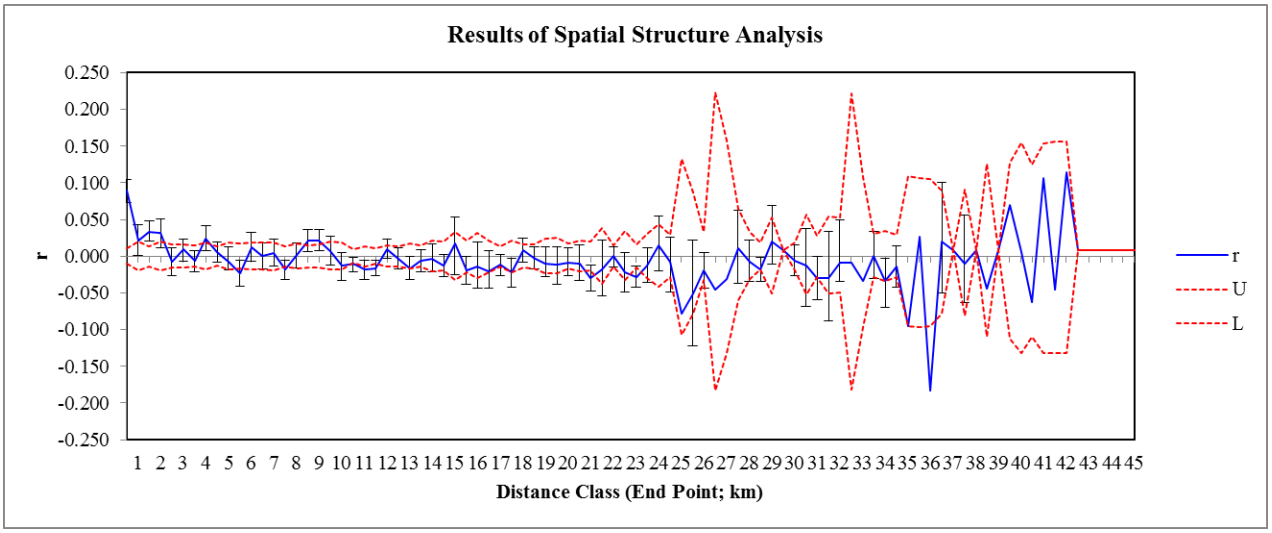

Figure 13: Individual codominant marker distance based on 14 loci is not autocorrelated to straight-line geographic distance at greater than 2.5 km, however there is slight autocorrelation at less than 3 km (GenAlEx; Peakall & Smouse 2006, 2012; Banks & Peakall 2012).

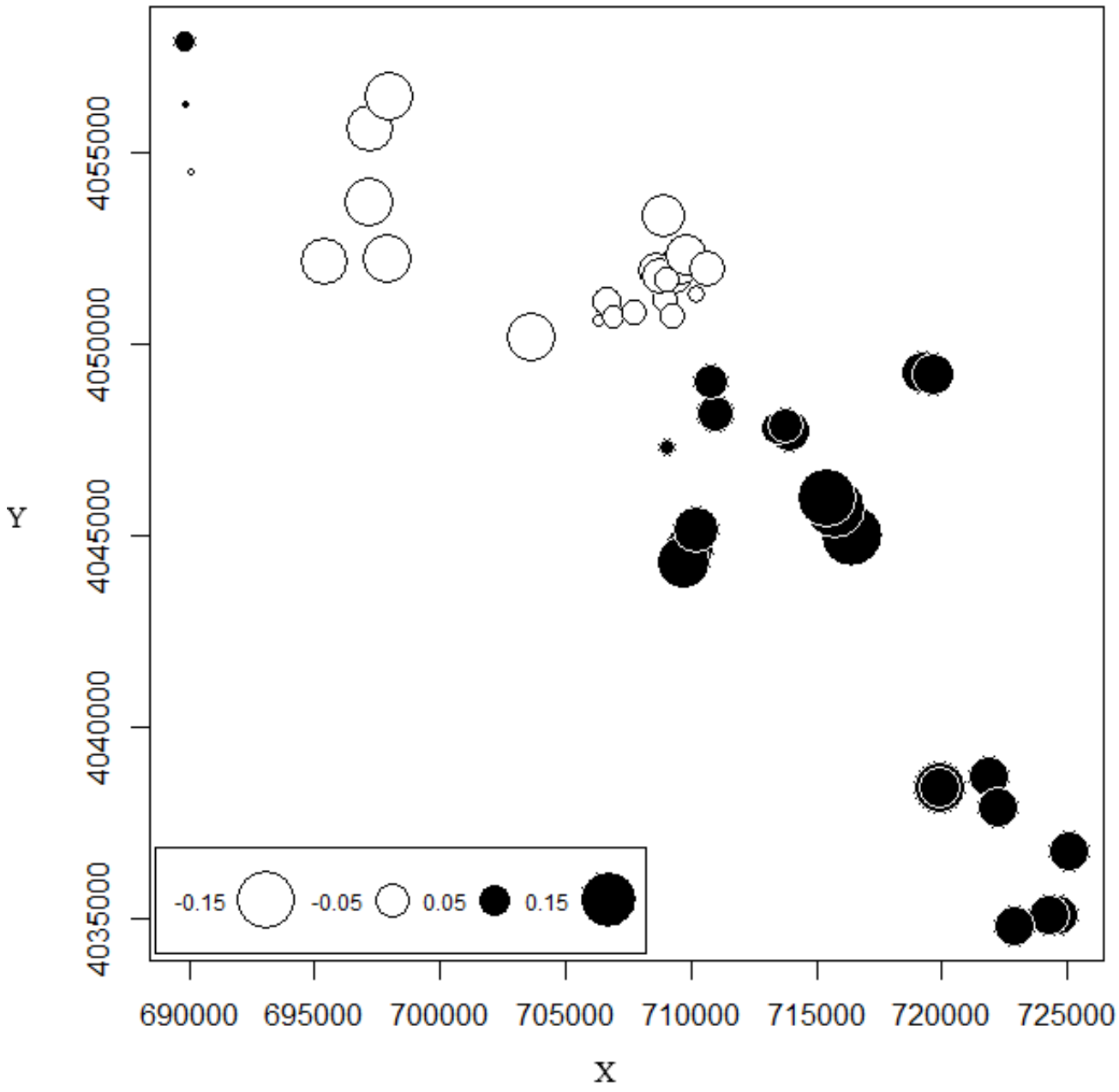

Figure 14: Genetic differences of individuals (n=121) across geographic space based on the first Moran eigenvector from a Dps distance matrix. Locus dst1318 was not used in the analysis. Circles of similar size and color denote genetically similar scoring of individuals on the first Moran eigenvector, with placement being geographic location (Universal Transverse Mercator Zone 10).

Dispersal

COLONY output identified 4 full-siblings (Probability ≥ 0.9, Figure 15-16, Table 3), and 31 half-siblings (10 at a probability≥ 0.95, 31 at a probability ≥ 0.9; Figure 15,Figure **17**, Table 3). No parent-offspring pairs were identified. A full-sibling pair was 5.52km apart and a half-sibling pair was 19.64 km apart, although most siblings (3 pairs) and half-siblings (12 pairs) were located at the same site. The inbreeding coefficient calculated with COLONY, analogous to Wright's F_{IS}, was estimated to be 0.109 for all 10 runs.

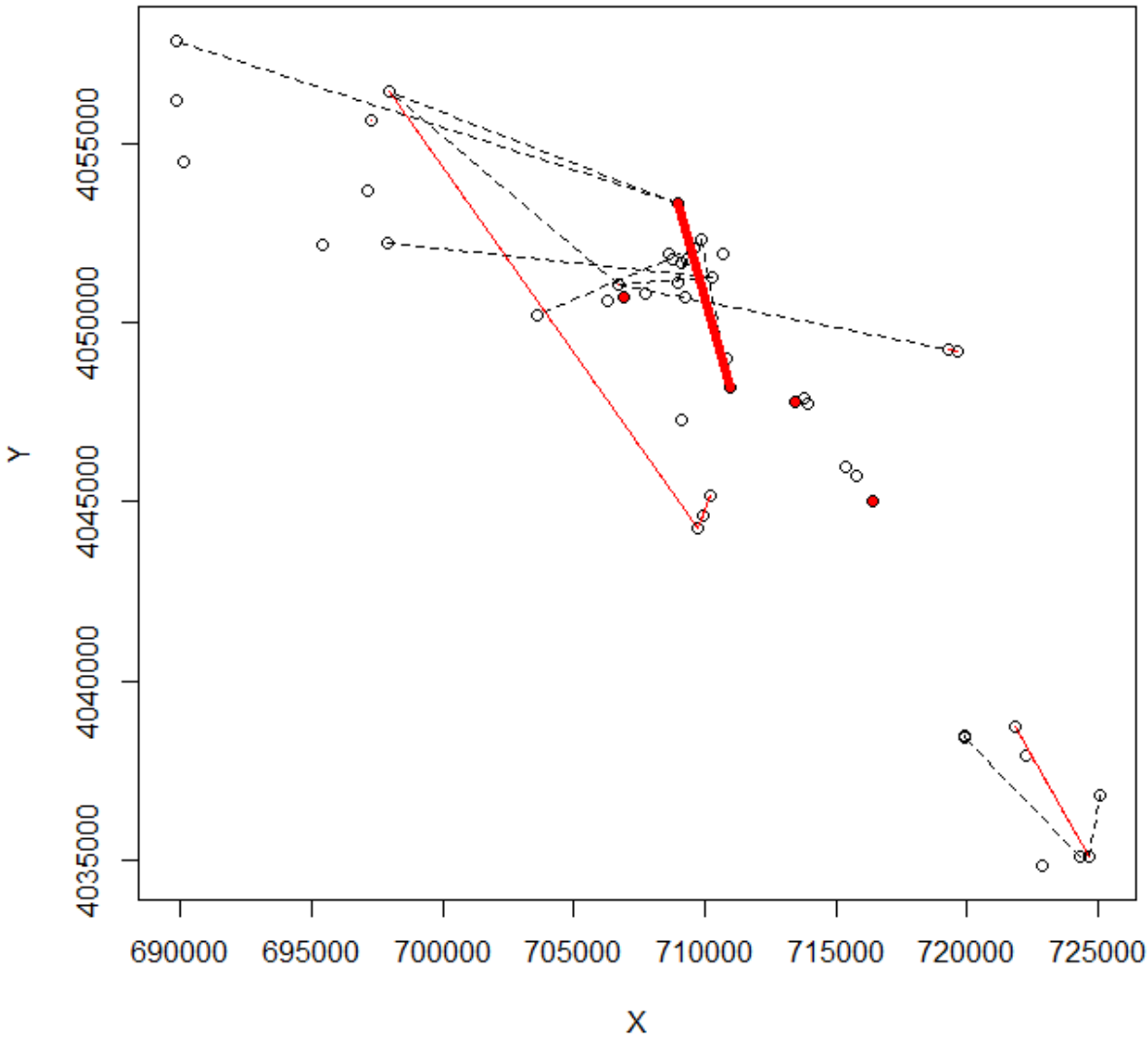

643

644 **Figure 15:** Geographic locations of half siblings identified (red thin line, n=10, probability ≥
645 0.95, black dotted line, n=21, probability: .95> probability ≥ .9) and full-siblings
646 identified (red thick line, n=4, probability ≥ 0.9), but only 1 full-sibling pair was caught
647 at different sites.

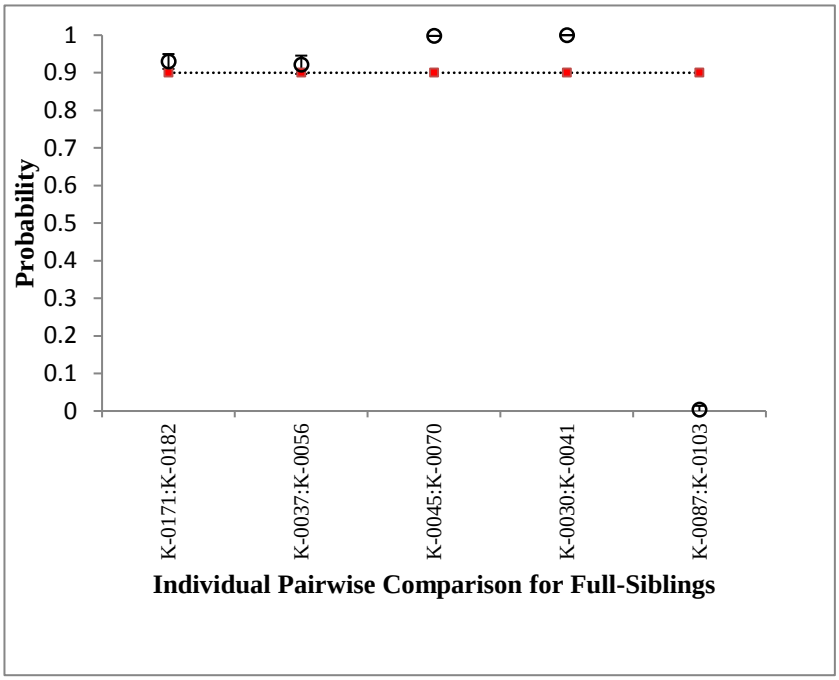

Figure 16: Pairwise full-sibling probabilities and standard deviations generated from 10 runs of COLONY with the threshold (probability=. 9) used to identify "true" full-siblings (red).

651 **Table 3:** GKR full-sibling and half-sibling pairs that were considered pairs with mean
652 probability of being related and standard deviation from 10 COLONY runs

Type	Pair ID	Distance (km)	Mean Probability	SD
Full-Siblings	K-0030:K-0041	0	1	0
	K-0045:K-0070	5.52	0.998	0
	K-0171:K-0182	0	0.93	0.019788
	K-0037:K-0056	0	0.9212	0.024399
Half-Siblings	K-0049:K-0069	0	0.9851	0.000316
	K-0067:K-0099	16.93	0.9836	0.000516
	K-0071:K-0081	1.02	0.9827	0.000483
	K-0046:K-0045	0	0.9717	0.001567
	K-0096:K-0105	0	0.971	1.17E-16
	K-0005:K-0029	4.56	0.9706	0.000966
	K-0047:K-0080	0.43	0.9699	0.003542
	K-0090:K-0096	0	0.969	0.001633
	K-0033:K-0230	0.39	0.9658	0.004686
	K-0027:K-0040	0	0.9626	0.001838
	K-0065:K-0078	0.73	0.9509	0.003213
	K-0099:K-0101	0	0.9479	0.000568
	K-0199:K-0076	4.27	0.9472	0.000919
	K-0038:K-0036	0	0.947	0.001414
	K-0005:K-0022	1.73	0.946	0.001414
	K-0093:K-0103	0	0.9415	0.002461
	K-0014:K-0026	0.28	0.9414	0.000966
	K-0159:K-0202	0	0.9404	0.000516
	K-0044:K-0082	13.35	0.9396	0.000699
	K-0091:K-0105	0	0.9352	0.000919
	K-0040:K-0230	0.38	0.9279	0.000994
	K-0046:K-0070	5.52	0.9275	0.002593
	K-0068:K-0103	11.42	0.9269	0.000568
	K-0062:K-0040	3.58	0.9252	0.001317
	K-0064:K-0095	3.58	0.9252	0.003458
	K-0074:K-0211	19.64	0.9243	0.002908
	K-0021:K-0024	5.5	0.9242	0.0027
	K-0072:K-0102	16.93	0.9129	0.005384
	K-0079:K-0156	6.28	0.9129	0.002183
	K-0034:K-0057	0	0.9096	0.002119
	K-0053:K-0069	0	0.9079	0.001663

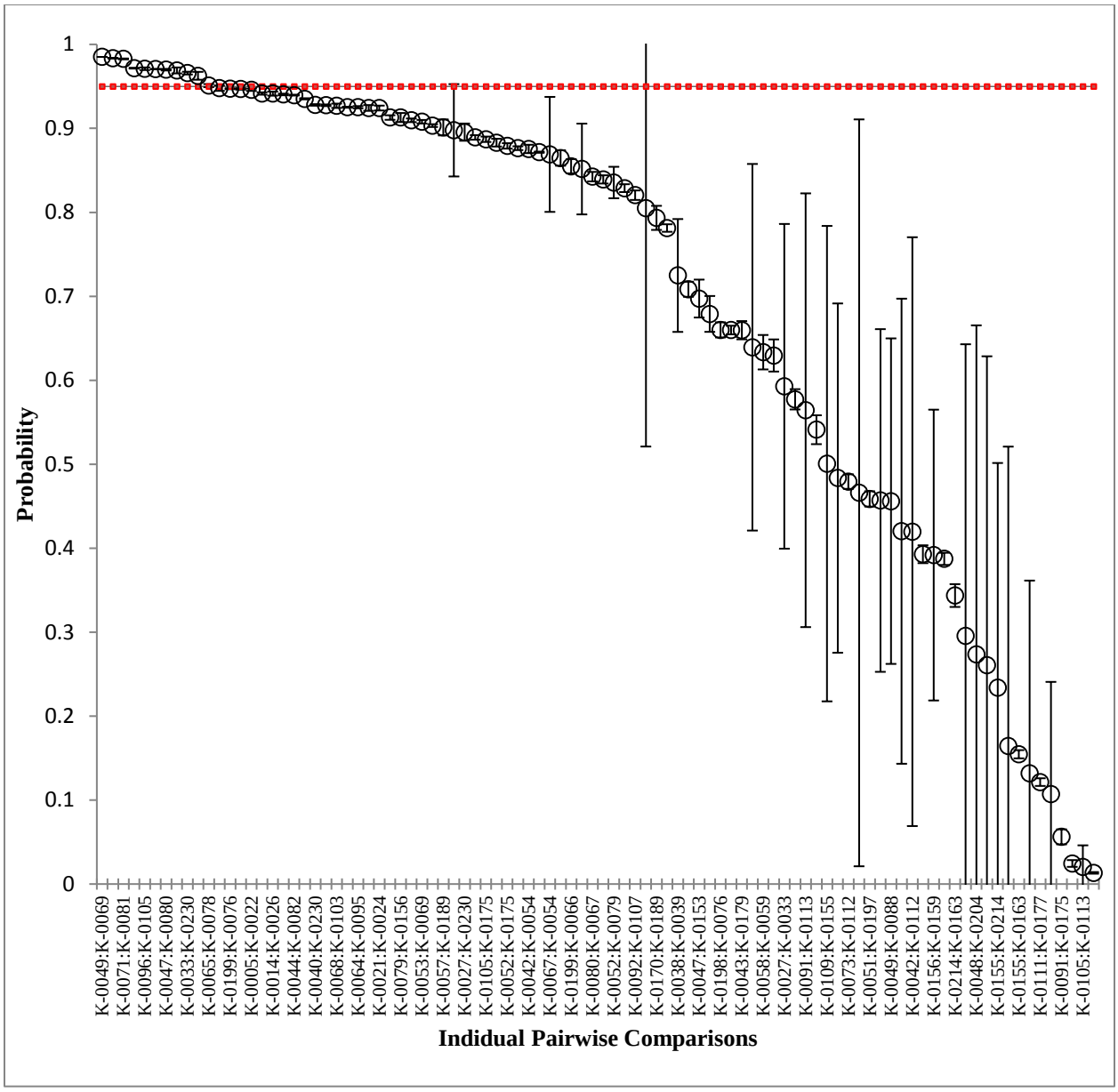

Figure 17: Pairwise half-sibling probabilities and standard deviations generated from 10 runs of COLONY with the threshold (probability= .95) used to identify "true" half-siblings (red).

Connectivity Modeling

For determining the impact landscape features have on connectivity, I identified from partial mantel tests that a slope greater than 10 degrees being assigned a high cost value compared to Dps was supported (mantel r=.14 p-value=.001; Table 4, Figure 18; mantel r = .09 p-value=.049;Figure 19). None of the parameters were significant when using the codominant marker distance genetic measure, although Slope Thresh 10 still had the highest mantel r (.0835) and lowest p-value (.096). Slope Thresh 10 was significant for both and could be considered significant at an α =.10 for codominant marker distance (p-value=.095). IBD models were both significant for the Dps and codominant marker distance genetic measures, with a mantel r correlation coefficient of .15 (p-value < .0011) and .10 (p-value < .001) respectively.

668 **Table 4:** Partial Mantel correlation for hypothesized costs of parameters for IBR. Isolation by
669 Distance measures are genetic distances correlated to the IBR null model using a mantel
670 test.

Genetic Measure	Model	Mantel *r*	p-value	Lower 2.5%	Upper 97.5%
Dps	**IBD**	**0.153351**	**1.00E-06**	**0.131578**	**0.177872**
	Slope Thresh 10	**0.139977**	**0.00102**	**0.10002**	**0.161762**
	Slope Thresh 5	0.044089	0.15175	0.006762	0.078341
	Slope Linear	0.042363	0.15926	0.005002	0.075853
	Precip Thresh 300	0.041233	0.16745	0.011026	0.070131
	Road Conductance	0.034128	0.21209	-0.00246	0.064995
	Road Resistance	0.025946	0.26657	-0.00778	0.050738
	Precip Linear	0.020414	0.31291	-0.01201	0.051841
	Veg Multi	-0.00113	0.52034	-0.03155	0.026602
	Precip Thresh 250-350	-0.03777	0.81256	-0.07193	-0.00243
	Veg Binary	-0.09476	0.99869	-0.12162	-0.06648
codominant	**IBD**	**0.109421**	**8.70E-05**	**0.086525**	**0.133708**
marker distance	Slope Thresh 10	0.083501	0.095827	0.023285	0.109809
	Veg Multi	0.027299	0.333785	-0.01203	0.062336
	Slope Linear	-0.00296	0.520168	-0.04967	0.03974
	Road Conductance	-0.00538	0.532345	-0.05098	0.035175
	Precip Linear	-0.01367	0.585784	-0.04866	0.022447
	Slope Thresh 5	-0.02291	0.638811	-0.06525	0.017844
	Precip Thresh 300	-0.02291	0.641697	-0.06846	0.020333
	Road Resistance	-0.02583	0.653235	-0.06055	0.015433
	Veg Binary	-0.08241	0.962575	-0.1238	-0.0467
	Precip Thresh 250-350	-0.10924	0.965256	-0.14445	-0.07567

671

672

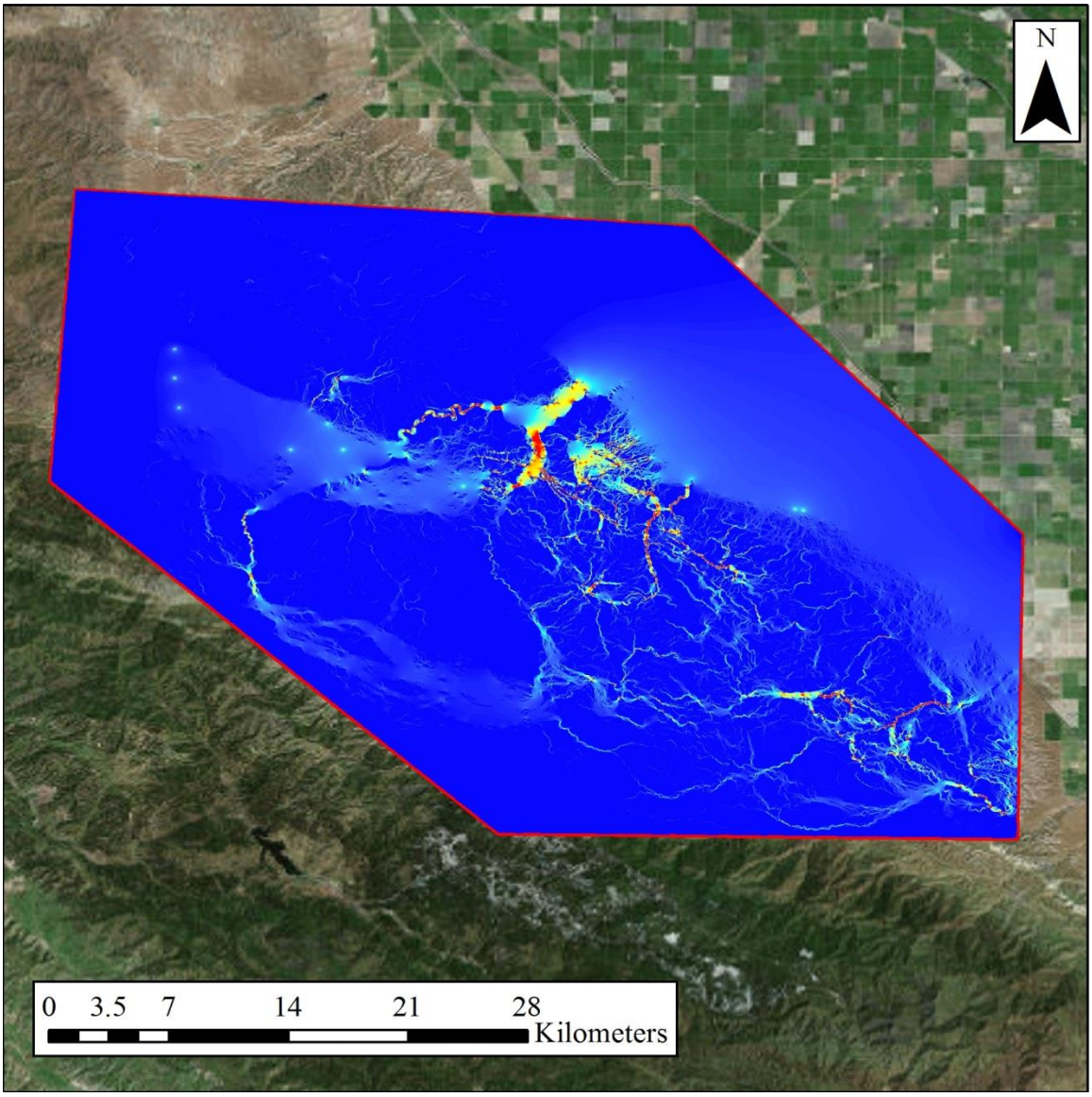

673

674 **Figure 18:** Current flow, or probability that an individual will pass through a pixel, identified for
675 pairwise distances in Circuitscape under the hypothesis that slope greater than 10 degrees
676 is a higher cost to movement than slope less than or equal to 10 degrees.

677

678

679 **Table 5:** Partial Mantel correlation for hypothesized costs of parameters for LCP. Isolation by
680 Distance measures are genetic distances correlated to the LCP null model using a mantel
681 test.

Genetic Measure	Model	Mantel *r*	p-value	Lower 2.5%	Upper 97.5%
Dps	**IBD**	**0.052731**	**0.031814**	**0.029944**	**0.078247**
	Slope Thresh 10	**0.093492**	**0.049198**	**0.048049**	**0.139047**
	Road Resistance	0.022115	0.287734	-0.01042	0.055803
	Veg Binary	0.01429	0.337588	-0.01211	0.044664
	Slope Linear	0.021515	0.349368	-0.01512	0.06094
	Slope Thresh 5	0.011569	0.417571	-0.02854	0.047469
	Veg Multi	0.008727	0.438278	-0.02621	0.060349
	Precip Thresh 300	-0.00189	0.503181	-0.04206	0.037026
	Road Conductance	-0.01874	0.608624	-0.05197	0.018198
	Precip Linear	-0.01765	0.628298	-0.04112	0.011597
	Precip Thresh 250-350	-0.06515	0.8528	-0.09886	-0.02472
codominant marker distance	**Slope Thresh 10**	**0.093492**	**0.049626**	**0.045272**	**0.135326**
	IBD	0.029189	0.229417	-0.00501	0.06003
	Road Resistance	0.022115	0.288058	-0.0107	0.058854
	Veg Binary	0.01429	0.33776	-0.01271	0.043933
	Slope Linear	0.021515	0.348309	-0.01468	0.066354
	Slope Thresh 5	0.011569	0.417526	-0.02413	0.04653
	Veg Multi	0.008727	0.437543	-0.03138	0.05798
	Precip Thresh 300	-0.00189	0.502502	-0.04072	0.036324
	Road Conductance	-0.01874	0.608949	-0.052	0.018259
	Precip Linear	-0.01765	0.628029	-0.0421	0.010988
	Precip Thresh 250-350	-0.06515	0.852552	-0.09945	-0.0241

682

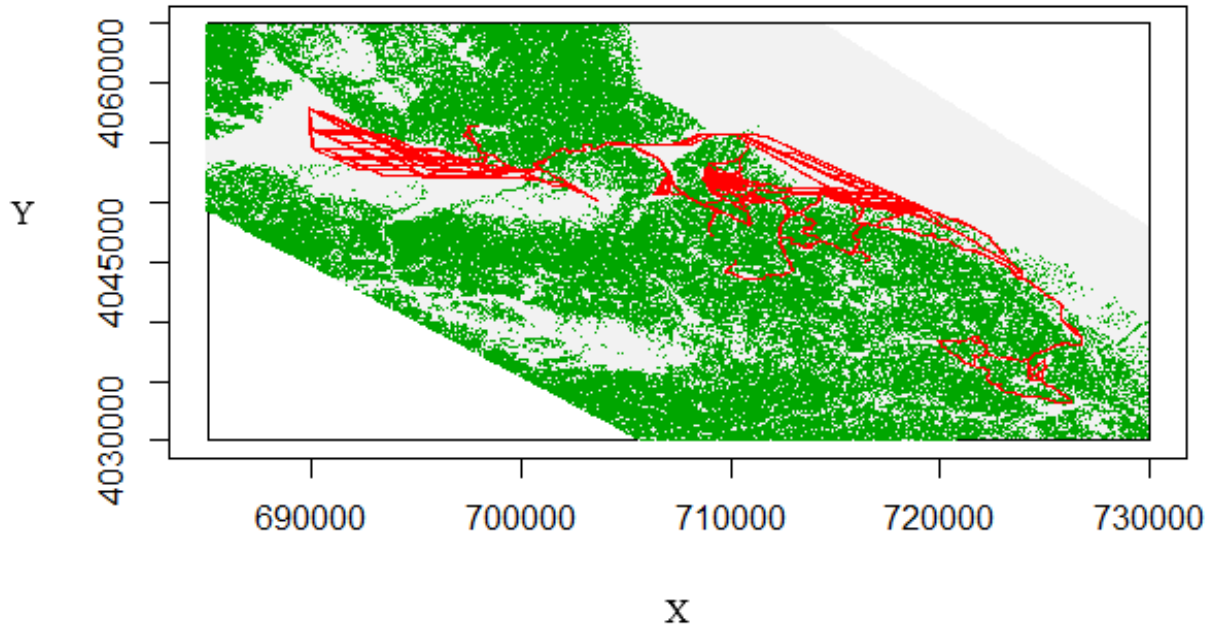

Figure 19: Least Cost Paths identified for pairwise distances in "ecodist" under the hypothesis that slope greater than 10 degrees is a higher cost to movement than slope less than or equal to 10 degrees.

For IBR and LCP with codominant marker distance, there were not enough significant models to conduct causal modeling. However, for LCP with Dps, causal modeling was used to determine significance. When all the significant models were offset by the most correlated model, none of the correlations were significant. The top model, offset by the initially significant models, was also not significant.

For individuals within 3km of each other, only Road Conductance, where non-roads had a higher cost than roads, was significantly correlated to genetic distances (mantel r = .062, p-value= .0357) although the correlation was small. Within 3km, IBD was significant for all cost measures, with the highest correlation being IBR with Dps (mantel r = .30, p-value < .001).

Discussion

In this study, I identified a single population adhering to IBD, which created three to four genetically weak clusters from TESS and STRUCTURE within the CPNA GKR metapopulation located in Panoche Valley, the Southern Ciervo Hills, and the Tumey Hills near the I-5 corridor. There is likely a fourth genetic subpopulation signature in the Panoche Hills. Distance followed by a threshold slope, where individuals can easily traverse if the slope is less than 10 degrees, best explained individual genetic distances, while precipitation, vegetation, roads, habitat suitability (MaxEnt) and non-linear models did not correlate significantly to individual genetic distances. Dps identified stronger and more correlations than codominant marker distance for giant kangaroo rats, and may capture more fine scale genetic structure than codominant marker distance.

Population Structure

The subpopulations identified seem to correlate to the Panoche Valley, Tumey Hills, and Ciervo Hills subpopulations identified by Good *et al.* (1997) and Loew *et al.* (2005). However, rather than being discrete subpopulations, these subpopulations appear to exist along clines with contact zones and overlap between the populations. Good *et al.* (1997) and Loew *et al.* (2005) trapped at discrete locations, whereas I trapped continuously throughout the CPNA, highlighting that what was previously thought as unique populations is more likely due to isolation by distance effects. TESS and STRUCTURE both provided reasonable interpretation of genetic clusters based on geographic location. The difference in identified subpopulations is partly due to STRUCTURE having 2 additional individuals that were caught within the more central populations, and STRUCTURE not being well suited to identify clinal genetic variation such as isolation by distance (Hubisz *et al.* 2009). Although STRUCTURE with the same individuals as

TESS identified 3 clusters, the admixture and credible intervals indicate that these are most likely not distinct subpopulations.

TESS clustered the population in the Northern Panoche Hills with the Panoche Valley population, whereas STRUCTURE determined that it was unique. Because TESS uses geographic distance derived from Delaunay triangulation as a prior, but does not take topological complexity into account, this population is most likely as distinct as the other subpopulations because it is isolated by steep slopes. Both TESS and STRUCTURE clustered individuals into a Panoche Valley subpopulation and a Ciervo Hills subpopulation, with a third subpopulation to the east, just west of Interstate 5, the Tumey Hills subpopulation. However, TESS and STRUCTURE show these 3 subpopulations intermingling in the Northern Tumey Hills, indicating contact zones. While the separate populations are in line with the observations made by Loew *et al.* (2005) and Good *et al.* (1997), these subpopulations may reflect kinship groups or weak genetic separation. STRUCTURE identified the same populations when related individuals were removed, but TESS did not. TESS may incorporate gradations more accurately than STRUCTURE. Because TESS clustered into a single population after related individuals were removed, the relatively high genetic admixture of individuals, and the apparent clinal genetic structure of GKR, STRUCTURE and TESS most likely recovered some level of kinship groups, or related individuals, without identifying demographically independent populations.

However, also of note is the temporal resolution that this clustering can inform. Good *et al.* (1997) used mtDNA haplotypes to identify their population structure, whereas Loew *et al.* (2005) and I used microsatellites. Because mtDNA mutates more slowly than microsatellites (Wang 2010; Epps & Keyghobadi 2015), and my collections were conducted 20 years later than Good *et al.* (1997), these clusters should be viewed as temporally stable populations. One

possibility is there are overlapping population boundaries from population range expansion post bottlenecks (Chen *et al.* 2007). If sampling occurred during population range expansion, there may be evidence that previously identified populations by Good *et al.* (1997) and Loew *et al.* (2005) are source populations.

With these clusters, we can also address the hypothesis that Panoche and Silver Creek act as barriers to dispersal. Because genetic grouping did not isolate individuals on either side of the rivers, it does not appear that the creeks act as a barrier. The results from STRUCTURE and TESS appear more indicative of a barrier by sampling design, where arbitrary boundaries and genetic clusters identified by the programs are representative of breaks in sampling rather than genetically isolated subpopulations (Ramey II *et al.* 2007). STRUCTURE identifies the highest level of genetic segregation present in the sample area (Evanno *et al.* 2005; Cercueil *et al.* 2007), and, when coupled with the probable Wahlund Effect from HWP testing, indicates that there may be further population subdivision into kinship groups at smaller scales based on the admixture of the entire population. This is further supported by the gradient landscape genetic structure shown by the Moran Eigenvector Map.

Dispersal

COLONY indicates that GKR are capable of large-scale movement not previously reported. A full-sibling pair was found 5.52 km apart, and 10 half-siblings were found from 0-19.64 km apart. Whereas the previously recorded maximum distance from Loew *et al.* (2005) was 700m, this observed increase is most likely due to difficulty noting natal and juvenile dispersal of burrowing rodents.

Genetic samples were obtained during drought years in California, and during “harsher” years, some species may become centralized in areas of high habitat suitability (Auger *et al.*

2016; Koen *et al.* 2016). Furthermore, dispersal is likely negatively related to density, where *Dipodomys* spp. will cohabitate burrows at high population density and disperse farther during population declines (Edelman 2011; Meshriy *et al.* 2011). By having this plasticity in social interactions and cues for dispersal, it may be that GKR dispersal is determined by demographics or at-site environmental parameters rather than between-site parameters. It is possible that satellite populations condensed into the areas of higher habitat suitability, or vice-versa where central populations emitted dispersers to satellite populations, convoluting genetic signature.

GKR Connectivity

Landscape resistance defined by a threshold slope was most correlated to GKR population structure after IBD, but it was a relatively weak correlation. While habitat models may estimate gene flow for certain species (e.g. Shafer *et al.* 2012), the MaxEnt model created here did not represent GKR connectivity well. While habitat suitability models may identify key habitat features for GKR abundance (Bean *et al.* 2014b), high abundances may negatively impact dispersal (Peterman *et al.* 2015), making habitat suitability models uninformative for GKR connectivity (see Mateo-Sánchez *et al.* 2015).

There did not appear to be a correlation between genetic distances and roads, either. Barrows *et al.*(2006) found that desert kangaroo rats (*Dipodomys deserti*) were negatively impacted by roads at a fine scale, hypothesizing that road grading and water runoff may compact soil. The response of kangaroo rats to roads may vary based on road type (e.g. paved, dirt, gravel; Brock & Kelt 2004), mortality risk (Barrows *et al.* 2006), or impact to social systems (Shier *et al.* 2012). Brehme *et al.* (2013) noted that Dulzura kangaroo rats (*Dipodomys simulans*) did not avoid roads, and suggested, though with small sample size, that dirt roads were more permeable than the surrounding habitat to kangaroo rats. In the CPNA, roads are predominantly

dirt roads that have limited access, although Little Panoche Road and part of Panoche Road are paved and have higher traffic. Roadkill GKR, Heermann kangaroo rats (*Dipodmoys heermanii*), and a McKittrick pocket mouse (*Perognathus inornatus neglectus*) have been observed along paved roads, indicating that mortality occurs at some level due to traffic.

With GKR, I identified 4 potential reasons why there is weak genetic signatures. GKR genetic signatures may be (1) GKR mating and dispersal behaviors, (2) driven by at-site ecological drivers than by between-site environments, (3) temporal and stochastic environmental variance, or (4) the statistics used to determine gene flow.

Mating and Dispersal Behavior

GKR and *Dipodomys* spp. have been noted to have a highly flexible social structure. Source-sink metapopulation dynamics can impact demography (Gundersen *et al.* 2001; Cosentino *et al.* 2014) without genetic effects (Cosentino *et al.* 2015).GKR demonstrate neighbor recognition (Murdock & Randall 2001) and have a variable mating and reproductive cycle [e.g. Meshriy *et al.* (2011) state the breeding season is March-April, but I found juveniles and a copulate plug in August], which might be the cause of low genetic variation, and low correlation to environmental predictors.

If GKR prefer to mate with known individuals (Murdock & Randall 2001), then the effects of environmental parameters on gene flow may be swamped by GKR mating behavior. Using IBR and LCP to understand the interaction between the landscape and GKR may violate the assumption of constant flow of individuals (Carroll *et al.* 2012), and large-scale dispersal may be just as or more variable as within site dispersal.

Finally, dispersal may be more of a "generalist" behavior for a habitat "specialist" rodent (Centeno-Cuadros *et al.* 2011; Peled *et al.* 2016). Peled *et al.* (2016) found that a habitat specialist gerbil had higher gene flow than a habitat generalist gerbil. GKR, while being habitat specialists, may be generalists during dispersal. Skvarla *et al.* (2004) found that habitat matrix had a low impact on connectivity of banner-tailed kangaroo rats (*Dipodomys spectabilis*), which seems consistent with my findings of GKR. If an organism relies on a specific habitat type, not responding to environmental factors during dispersal could be adaptive for colonization of fragmented habitats (Centeno-Cuadros *et al.* 2011).

At-Site Ecological Drivers

It appears difficult to see any distance metric that would explain genetic variance well. The genetic composition observed from STRUCTURE may be more influenced by patch size than gene flow between patches and patch configuration (Cushman *et al.* 2012; Jackson & Fahrig 2016). Overlapping generations decrease the impact of genetic drift, and the genetic composition may be driven by effective population size (Ne) rather than connectivity.

Genetic distances account for the colonization history and drift as well as connectivity (Marko & Hart 2011; Moilanen 2011). Because drift is a function of effective population size (Ne), and most connectivity studies don't include demographics, Ne can vary across the landscape, with that variance being attributed to dispersal costs (Richardson *et al.* 2016; Waits & Storfer 2016). Busch et al. (2007) did not see a signature of genetic bottlenecking after a severe demographic decline in banner-tailed kangaroo rats. Even if alleles are lost during population declines, the increase in long-distance dispersers during these events may act as an offset. With quick replacement of alleles, the number of rare alleles will remain constant and there will be not

be a genetic signature of a mode shift (Busch *et al.* 2007). Cosentino *et. al* (2014; 2015) determined that banner-tailed kangaroo rat demographics were influenced by connectivity, but that founder effect or colonization genetic structure was not present.

Stochastic Environment

GKR may be evolutionarily adapted to highly stochastic environments, which is reflected in their plastic mating systems and dispersal. This high level of variance in dispersal and social arrangement may be indicative of large scale gene flow variance due to temporal effects on environmental parameters, and response to environment may not be apparent with high stochasticity in environmental pressures (Sexton *et al.* 2014). The variance in climatic and weather conditions may correlate to GKR impact on arid grassland communities (Prugh & Brashares 2012), and this highly variable climate most likely impacts dispersal as well. Kangaroo rats also have temporal and spatial responses to vegetation and available food, including temporal species composition shifts (Auger *et al.* 2016; Bean *et al.* 2016), as well as precipitation (Thibault *et al.* 2010); dominant vegetation can vary from year to year due to timing of rainfall (Bartolome *et al.* 2007), and green-ups of vegetation can increase reproductive success in *Dipodomys* spp. (Grinnell 1932; Lightfoot *et al.* 2012). Precipitation thus creates stochastic boom and bust dynamics in food availability. This stochastic environment could mean that the static conditions used in creating the cost maps do not accurately represent the current pressures on dispersal because the environmental limitation on dispersal changes from year to year. While slope and road presence are most likely constant, the precipitation regime and vegetation community may not be indicative of current pressures.

Statistics

Mantel tests and partial mantel tests depend on identifying linear relationships between environmental cost distances and genetic distances, and if the environment is too heterogeneous (Legendre & Fortin 2010; Kierepka & Latch 2015), not fragmented enough, or costs aren't variable enough, mantel tests may perform poorly (Zeller *et al.* 2016). If there is an inconsistent genetic response to environmental distances, mantel tests may not accurately identify influential landscape features (Keller *et al.* 2013; Legendre *et al.* 2015), and this was observed with the increase in IBD correlation at 3km compared to IBD for the full extent of the study area. However, causal modeling tends to be robust at identifying influential parameters (Castillo *et al.* 2014; Mateo-Sánchez *et al.* 2015). Causal modeling also probably performed poorly due to lack variation between some models (Zeller *et al.* 2016), so if one was offset by a model of the same parameters at different powers, there was probably high correlation and they explained similar variance. Also, most connectivity studies, including this one, analyze connectivity over one landscape, and, without repetition across areas, it is difficult to draw general conclusions (Short Bull *et al.* 2011).

There are also inherent pitfalls of using genetic data; Orozco-Ter-Wengel *et al.* (2011) found that genetic signatures varied when less than 30 microsatellites were used. Along with this, while the field of landscape genetics has been growing and novel landscape modeling techniques have been developed, a genetic measure specific to determine connectivity is still lacking (Waits & Storfer 2016).

LCP identified 36 models with a p-value<.05, although the mantel *r* correlations were less than 0.1, indicating that while correlation was statistically significant, the environmental parameters were not highly correlated to the genetic distances. IBR had a higher correlation to

genetic distances than LCP. This suggests that GKR use multiple pathways for dispersal across the study area, and is most likely due to homogenous habitat between individuals in the respective valleys. In addition, Slope Thresh 10 identified Panoche Creek as a potential area of high dispersal probability for both IBR and LCP.

Management Implications

GKR are a species requiring careful management considerations, for a solar farm in the CPNA is currently under construction and climate change may require GKR to move to new areas where they were not historically present. First, there are no identified gene flow barriers between occupied sites, and the genetic structure identified by STRUCTURE and TESS should be considered as Isolation by Distance effects rather than as genetically distinct populations. Connectivity is an important consideration for both of the potentially fragmenting effects of solar farms and climate change on GKR populations. GKR dispersal in the CPNA is not strongly impacted by environmental parameters, and the sibling/halfsibling results of COLONY tend to support that this is due to high mobility rather than an artifact of sampling extent. I identified a full-sibling pair that was 5.52 km apart, whereas previous literature on GKR dispersal identified a max distance of .7 km with a mean around .1km. GKR should be able to recolonize extinct patches as long as there are source populations emitting dispersers, thus node-centric connectivity estimates should be considered.

While the population structure, dispersal, and connectivity of GKR all align with an isolation by distance population, connectivity and population genetics are only part of the picture, and management should be determined based off of the full life history of GKR. For GKR, continued persistence will most likely depend on suitable habitat availability, and GKR

habitat protection and creation will be the driving actions for species persistence, although it is worth noting that anthropogenic barriers to dispersal aside from roads were not considered.

Literature Cited

Adriaensen F, Chardon JP, De Blust G *et al.* (2003) The application of "least-cost" modelling as a functional landscape model. *Landscape and Urban Planning*, **64**, 233–247.

Alagador D, Triviño M, Cerdeira JO *et al.* (2012) Linking like with like: Optimising connectivity between environmentally-similar habitats. *Landscape Ecology*, **27**, 291–301.

Anderson EC, Dunham KK (2008) The influence of family groups on inferences made with the program Structure. *Molecular ecology resources*, **8**, 1219–29.

Auger J, Meyer SE, Jenkins SH (2016) a mast-seeding desert shrub regulates population dynamics and behavior of its heteromyid dispersers. *Ecology and Evolution*, **6**, 2275–2296.

Balkenhol N, Holbrook JD, Onorato D *et al.* (2014) A multi-method approach for analyzing hierarchical genetic structures: A case study with cougars Puma concolor. *Ecography*, **37**, 552–563.

Balloux F, Lugon-Moulin N (2002) The estimation of population differentiation with microsatellite markers. *Molecular Ecology*, **11**, 155–165.

Banks SC, Peakall R (2012) Genetic spatial autocorrelation can readily detect sex-biased dispersal. *Molecular Ecology*, **21**, 2092–2105.

Barrows CW, Allen MF, Rotenberry JT (2006) Boundary processes between a desert sand dune community and an encroaching suburban landscape. *Biological Conservation*, **131**, 486–494.

Bartolome JW, Barry WJ, Griggs T, Hopkinson P (2007) Valley Grassland. In: *California grasslands: ecology and management*, pp. 371–397.

Bean WT (2012) Spatial ecology of the giant kangaroo rat (Dipodomys ingens): a test of species distribution models as ecological revealers. UC Berkeley.

Bean WT, Alexander N, Westphal M (2016) Drought-related giant kangaroo rat decline in the Ciervo-Panoche. In: *The Western Section of the Wildlife Society*, p. Poster.

Bean WT, Prugh LR, Stafford R *et al.* (2014a) species distribution models of an endangered rodent offer conflicting measures of habitat quality at multiple scales. *Journal of Applied Ecology*, **51**, 1116–1125.

Bean WT, Stafford R, Butterfield HS, Brashares JS (2014b) A multi-scale distribution model for non-equilibrium populations suggests resource limitation in an endangered rodent. *PlosOne*, **9**, e106638.

Benjamini Y, Hochberg Y (1995) Controlling the false discovery rate: a practical and powerful approach to multiple testing. *Journal of the Royal Statistical Society*, **57**, 289–300.

Biek R, Real LA (2010) The landscape genetics of infectious disease emergence and spread. *Molecular ecology*, **19**, 3515–31.

940 Blackhawk NC, Germano DJ, Smith PT (2016) Genetic variation among population of the
941 endangered giant kangaroo rat, Dipodomys ingens, in the Southern San Joaquin Valley. *The*
942 *American Midland Naturalist*, **175**, 261–274.

943 Blair ME, Melnick DJ (2012) Scale dependent effects of a heterogeneous landscape on genetic
944 differentiation in the Central American Squirrel Monkey (Saimiri oerstedii). *PlosOne*, **7**,
945 e43027.

946 Borcard D, Legendre P (2002) All-scale spatial analysis of ecological data by means of principal
947 coordinates of neighbour matrices. *Ecological Modelling*, **153**, 51–68.

948 Bowcock AM, Ruiz-Linares A, Tomfohrde J *et al.* (1994) High resolution of human evolutionary
949 trees with polymorphic microsatellites. *Nature*, **368**, 455–457.

950 Brehme CS, Tracey JA, McClenaghan LR, Fisher RN (2013) Permeability of roads to movement
951 of scrubland lizards and small mammals. *Conservation Biology*, **27**, 710–720.

952 Brock RE, Kelt DA (2004) Influence of roads on the endangered Stephens' kangaroo rat
953 (Dipodomys stephensi): are dirt and gravel roads different? *Biological Conservation*, **118**,
954 633–640.

955 Burnham KP, Anderson DR (2002) *Model Selection and Multimodel Inference: A Practical*
956 *Information-Theoretic Approach (2nd ed)*.

957 Busch JD, Waser P, DeWoody A (2007) Recent demographic bottlenecks are not accompanied
958 by a genetic signature in banner-tailed kangaroo rats (Dipodomys spectabilis). *Molecular*
959 *Ecology*, **16**, 2450–2462.

960 Carroll C, Mcrae BH, Brookes A (2012) Use of Linkage Mapping and Centrality Analysis
961 Across Habitat Gradients to Conserve Connectivity of Gray Wolf Populations in Western
962 North America. *Conservation Biology*, **26**, 78–87.

963 Castillo JA, Epps CW, Davis AR, Cushman SA (2014) Landscape effects on gene flow for a
964 climate-sensitive montane species, the American pika. *Molecular Ecology*, **23**, 843–856.

965 Centeno-Cuadros A, Romàn J, Delibes M, Godoy JA (2011) Prisoners in their habitat?
966 Generalist dispersal by habitat specialists: a case study in southern water vole (Arvicola
967 sapidus). *PlosOne*, **6**, e24613.

968 Cercueil A, François O, Manel S (2007) The genetical bandwidth mapping: a spatial and
969 graphical represetnation of population genetic structure based on the Wombling method.
970 *Theoretical Population Biology*, **71**, 332–341.

971 Chen C, Durand E, Forbes F, François O (2007) Bayesian clustering algorithms ascertaining
972 spatial population structure: A new computer program and a comparison study. *Molecular*
973 *Ecology Notes*, **7**, 747–756.

974 Clobert J, Le Galliard J-F, Cot J, Meylan S, Massot M (2009) Informed dispersal, heterogeneity
975 in animal dispersal syndromes and the dynamics of spatially structure populations. *Ecology*
976 *Letters*, **12**, 197–209.

977 Cooper LD, Randall JA (2007) Seasonal changes in home ranges of the giant kangaroo rat
978 (Dipodomys ingens): a study of flexible social structure. *Journal of Mammalogy*, **88**, 1000–
979 1008.

980 Corander J, Waldmann P, Sillanpää MJ (2003) Bayesian analysis of genetic differentiation
981 between populations. *Genetics*.

982 Cosentino BJ, Schooley RL, Bestelmeyer BT, Kelly JF, Coffman JM (2014) Constraints and
983 time lags for recovery of a keystone species (Dipodomys spectabilis) after landscape
984 restoration. *Landscape Ecology*, **29**, 665–675.

985 Cosentino BJ, Schooley RL, Bestelmeyer BT, McCarthy AJ, Sierzega K (2015) Rapid genetic
986 restoration of a keystone species exhibiting delayed demographic response. *Molecular*
987 *Ecology*, **24**, 6120–6133.

988 Coulon A, Guillot G, Cosson J-F *et al.* (2006) Genetic structure is influenced by landscape
989 features: empirical evidence from a roe deer population. *Molecular ecology*, **15**, 1669–1679.

990 Cushman SA, Shirk A, Landguth EL (2012) Separating the effects of habitat area, fragmentation
991 and matrix resistance on genetic differentiation in complex landscapes. *Landscape Ecology*,
992 **27**, 369–380.

993 Cushman SA, Wasserman TN, Landguth EL, Shirk AJ (2013) Re-evaluating causal modeling
994 with mantel tests in landscape genetics. *Diversity*, **5**, 51–72.

995 Edelman AJ (2011) Sex-specific effects of size and condition on timing of natal dispersal in
996 kangaroo rats. *Behavioral Ecology*, **22**, 776–783.

997 Elliot NB, Cushman SA, Macdonald DW, Loveridge AJ (2014) The devil is in the dispersers:
998 Predictions of landscape connectivity change with demography. *Journal of Applied*
999 *Ecology*.

1000 Epperson BK, Li T-Q (1997) Gene dispersal and spatial genetic structure. *Evolution*, **51**, 672–
1001 681.

1002 Epps CW, Keyghobadi N (2015) Landscape genetics in a changing world: disentangling
1003 historical and contemporary influences and inferring change. *Molecular Ecology*, **24**, 6021–
1004 6040.

1005 Epps CW, Wasser SK, Keim JL, Mutayoba BM, Brashares JS (2013) Quantifying past and
1006 present connectivity illuminates a rapidly changing landscape for the African elephant.
1007 *Molecular Ecology*, **22**, 1574–1588.

1008 Evanno G, Regnaut S, Goudet J (2005) Detecting the number of clusters of individuals using the
1009 software STRUCTURE: A simulation study. *Molecular Ecology*, **14**, 2611–2620.

1010 Falush D, Stephens M, Pritchard JK (2003) Inference of population structure using multilocus
1011 genotype data: linked loci and correlated allele frequencies. *Genetics*, **164**, 1567–1587.

1012 Ficetola GF, Garner TWJ, De Bernardi F (2007) Genetic diversity, but not hatching success, is

jointly affected by postglacial colonization and isolation in the threatened frog, Rana latastei. *Molecular Ecology*, **16**, 1787–1797.

Francis RM (2016) POPHELPER: an R package and web app to analyse and visualize population structure. *Molecular Ecology Resources*, doi: 10.1111/1755-0998.12509.

François O, Durand E (2010) Spatially explicit Bayesian clustering models in population genetics. *Molecular Ecology Resources*, **10**, 773–784.

Frye RJ (1983) Experimetnal field evidence of interspecific aggression between two species of kangaroo rat (Dipodomys). *Oecologia*, **59**, 74–78.

Galpern P, Peres-Neto PR, Polfus J, Manseau M (2014) MEMGENE: Spatial pattern detection in genetic distance data. *Methods in Ecology and Evolution*, **5**, 1116–1120.

GBIF.org (11th September 2016) GBIF Occurrence Download http://doi.org/10.15468/dl.o8x3ww

Germano DJ (2010) survivorship of translocated kangaroo rats in the San Joaquin Valley, California. *California Fish and Game*, **96**, 82–89.

Germano DJ, Rathbun GB, Saslaw LR (2001) Managing exotic grasses and conserving declining species. *Wildlife Society Bulletin*, **29**, 551–559.

Germano DJ, Rathbun GB, Saslaw LR *et al.* (2011) The San Joaquin Desert of California: ecologically misunderstood and overlooked. *Natural Areas Journal*, **31**, 138–147.

Good S, Williams D, Ralls K, Fleischer R (1997) Population structure of Dipodomys ingens (Heteromyidae): the role of spatial heterogeneity in maintaining genetic diversity. *Evolution*, **51**, 1296–1310.

Goslee SC, Urban DL (2007) The ecodist package for dissimilarity-based analysis of ecological data. *Journal Of Statistical Software*, **22**, 1–19.

Grinnell J (1932) Habitat relations of the giant kangaroo rat. *Journal of Mammalogy*, **13**, 305–320.

Gundersen G, Johannesen E, Andreassen HP, Ims RA (2001) Source-sink dynamics: how sinks affect demography of sources. *Ecology Letters*, **4**, 14–21.

Hamilton GS, Mather PB, Wilson JC (2006) Habitat heterogeneity influences connectivity in a spatially structured pest population. *Journal of Applied Ecology*, **43**, 219–226.

Harris RD, Palermo L, Tiller RL (1987) Effects of anthropogenic disturbances on habitat of giant kangaroo rats (Dipodomys ingens). *Endangered and Sensitive Species of the San Joaquin Valley, California Their Biolgoy, Management and Conservation*, 119–127.

Hawbecker AC (1944) The giant kangaroo rat and sheep forage. *Journal of Wildlife Management*, **8**, 161–165.

Hijmans RJ (2015) Introduction to the ' raster ' package (version 2 . 3-12). , 1–27.

1048 Holderegger R, Kamm U, Gugerli F (2006) Adaptive vs. neutral genetic diversity: Implications
1049 for landscape genetics. *Landscape Ecology*.

1050 Holyoak M, Casagrandi R, Nathan R, Revilla E, Spiegel O (2008) Trends and missing parts in
1051 the study of movement ecology. *Proceedings of the National Academy of Sciences of the*
1052 *United States of America*, **105**, 19060–5.

1053 Hubisz MJ, Falush D, Stephens M, Pritchard JK (2009) Inferring weak population structure with
1054 the assistance of sample group information. *Molecular Ecology Resources*, **9**, 1322–1332.

1055 Jackson ND, Fahrig L (2016) Habitat amount, not habitat configuration, best predicts population
1056 genetic structure in fragmented landscapes. *Landscape Ecology*, **31**, 951–968.

1057 Jakobsson M, Rosenberg NA (2007) CLUMPP: A cluster matching and permutation program for
1058 dealing with label switching and multimodality in analysis of population structure.
1059 *Bioinformatics*, **23**, 1801–1806.

1060 Jay F, Blum MGB, Frichot E, François O (2011) Modèles à variables latentes en génétique des
1061 populations. *Société Française de Statistique*, **152**, 3–20.

1062 Jenkins DG, Care M, Czerniewska J *et al.* (2010) A meta-analysis of isolation by distance: relic
1063 or reference standard for landscape genetics? *Ecography*, **33**, 316–320.

1064 Jombart T, Devillard S, Dufour A-B, Pontier D (2008) Revealing cryptic spatial patterns in
1065 genetic variability by a new multivariate method. *Heredity*, **101**, 92–103.

1066 Jones OR, Wang J (2010) COLONY: a program for parentage and sibship inference from
1067 multilocus genotype data. *Molecular Ecology Resources*, **10**, 551–555.

1068 Keller D, Holderegger R, Van Strien MJ (2013) Spatial scale affects landscape genetic analysis
1069 of a wetland grasshopper. *Molecular Ecology*, **22**, 2467–2482.

1070 Kershenbaum A, Blank L, Sinai I *et al.* (2014) Landscape influences on dispersal behaviour: A
1071 theoretical model and empirical test using the fire salamander, Salamandra infraimmaculata.
1072 *Oecologia*, **175**, 509–520.

1073 Kierepka EM, Latch EK (2015) Performance of partial statistics in individual-based landscape
1074 genetics. *Molecular Ecology Resources*, **15**, 512–525.

1075 Koen EL, Bowman J, Walpole AA (2012) The effect of cost surface paramterization on
1076 landscape resistance estimates. *Molecular Ecology Resources*, **12**, 686–696.

1077 Koen EL, Bowman J, Wilson PJ (2016) Node-based measures of connectivity in genetic
1078 networks. *Molecular Ecology Resources2*, **16**, 69–79.

1079 Landguth EL, Fedy BC, Oyler-McCance SJ *et al.* (2012) Effects of sample size, number of
1080 markers, and allelic richness on the detection of spatial genetic pattern. *Molecular Ecology*
1081 *Resources*, **12**, 276–284.

1082 Laurence S, Smith MJ, Schulte-Hostedde AI (2013) Effects of structural connectivity on fine
1083 scale population genetic structure of muskrat, Ondatra zibethicus. *Ecology and Evolution*, **3**,

3524–3535.

Legendre P, Fortin M-J (2010) Comparison of the Mantel test and alternative approaches for detecting complex multivariate relationships in the spatial analysis of genetic data. *Molecular Ecology Resources*, **10**, 831–844.

Legendre P, Fortin M-J, Borcard D (2015) Should the Mantel test be used in spatial analysis? *Methods in Ecology and Evolution*, **6**, 1239–1247.

Lightfoot DC, Davidson AD, Parker DG, Hernández L, Laundré JW (2012) Bottom-up regulation of desert grassland and shrubland rodent communities: implications of species-specific reproductive potentials. *Journal of Mammalogy*, **93**, 1017–1028.

Loew SS, Williams DF, Ralls K, Pilgrim K, Fleischer RC (2005) Population structure and genetic variation in the endangered giant kangaroo rat (Dipodomys ingens). *Conservation Genetics*, **6**, 495–510.

Lookingbill TR, Gardner RH, Ferrari JR, Keller CE (2010) Combining a dispersal model with network theory to assess habitat connectivity. *Ecological Applications*, **20**, 427–441.

Lugon-Moulin N, Hausser J (2002) Phylogeographical structure, postglacial recolonization and barriers to gene flow in the distinctive Valais chromosome race of the common shrew (Sorex araneus). *Molecular Ecology*, **11**, 785–794.

Manel S, Gaggiotti OE, Waples RS (2005) Assignment methods: matching biological questions with appropriate techniques. *TREE*, **20**, 136–142.

Mantel N (1967) The detection of disease clustering and a generalized regression approach. *Cancer Research*, **27**, 209–220.

Marko PB, Hart MW (2011) The complex analytical landscape of gene flow inference. *Trends in Ecology and Evolution*, **26**, 448–456.

Mateo-Sánchez MC, Balkenhol N, Cushman S *et al.* (2015) A comparative framework to infer landscape effects on population genetic structure: are habitat suitability models effective in explaining gene flow? *Landscape Ecology*.

McRae BH, Beier P (2007) Circuit theory predicts gene flow in plant and animal populations. *Proceedings of the National Academy of Sciences of the United States of America*, **104**, 19885–19890.

McRae B, Dickson B, Keitt T, Shah V (2008) Using circuit theory to model connectivity in ecology, evolution, and conservation. *Ecology*, **89**, 2712–2724.

McRae B, Shah V, Mohapatra T (2013) CIRCUITSCAPE User Guide. *The Nature Conservancy*, 28.

Meshriy MG, Randall JA, Parra L (2011) Kinship associations of a solitary rodent, Dipodomys ingens, at fluctuating population densities. *Animal Behaviour*, **82**, 643–650.

Moilanen A (2011) On the limitations of graph-theoretic connectivity in spatial ecology and

conservation. *Journal of Applied Ecology*, **48**, 1543–1547.

Munshi-South J (2012) Urban landscape genetics: Canopy cover predicts gene flow between white-footed mouse (Peromyscus leucopus) populations in New York City. *Molecular Ecology*.

Murdock HG, Randall JA (2001) Olfactory communication and neighbor recognition in giant kangaroo rats. *Ethology*, **107**, 149–160.

Nathan R (2001) The challenges of studying dispersal. *Trends in ecology & evolution*, **16**, 481–483.

Nathan R, Getz WM, Revilla E *et al.* (2008) A movement ecology paradigm for unifying organismal movement research. *Proceedings of the National Academy of Sciences of the United States of America*, **105**, 19052–9.

Naujokaitis-Lewis IR, Rico Y, Lovell J, Fortin M-J, Murphy MA (2013) Implications of incomplete networks on estimation of landscape genetic connectivity. *Conservation Genetics*, **14**, 287–298.

Nobert BR, Merrill EH, Pybus MJ, Bollinger TK, Hwang Y Ten (2016) Landscape connectivity predicts chronic wasting disease risk in Canada. *Journal of Applied Ecology*.

Orozco-Ter-Wengel P, Corander J, SchlÖtterer C (2011) Genealogical lineage sorting leads to significant, but incorrect Bayesian multilocus inference of population structure. *Molecular Ecology*, **20**, 1108–1121.

Parks SA, Mckelvey KS, Schwartz MK (2013) Effects of Weighting Schemes on the Identification of Wildlife Corridors Generated with Least-Cost Methods. *Conservation Biology*, **27**, 145–154.

Peakall R, Smouse PE (2006) GENALEX 6: Genetic analysis in Excel. Population genetic software for teaching and research. *Molecular Ecology Notes*.

Peakall R, Smouse PE (2012) GenAlEx 6.5: genetic analysis in Excel. Population Genetic software for teaching and research-an update. *Bioinformatics*, **28**, 2537–2539.

Peled E, Shanas U, Granjon L, Ben-Shlomo R (2016) Connectivity in fragmented landscape: generalist and specialist gerbils show unexpected gene flow patterns. *Journal of Arid Environments*, **125**, 88–97.

Peterman WE, Anderson TL, Ousterhout BH *et al.* (2015) Differential dispersal shapes population structure and patterns of genetic differentiation in two sympatric pond breeding salamanders. *Conservation Genetics*, **15**, 59–69.

Pflüger FJ, Balkenhol N (2014) A plea for simultaneously considering matrix quality and local environmental conditions when analysing landscape impacts on effective dispersal. *Molecular Ecology*, **23**, 2146–2156.

Phillips SB, Aneja VP, Kang D, Arya SP (2006) Modelling and analysis of the atmospheric

1156 nitrogen deposition in North Carolina. *International Journal of Global Environmental*
1157 *Issues*, **6**, 231–252.

1158 Pritchard JK, Stephens M, Donnelly P (2000) Inference of population structure using multilocus
1159 genotype data. *Genetics*, **155**, 945–959.

1160 Prugh LR, Brashares JS (2012) Partitioning the effects of an ecosystem engineer: kangaroo rats
1161 control community structure via multiple pathways. *Journal of Animal Ecology*, **81**, 667–
1162 678.

1163 Ramey II RR, Wehausen JD, Liu H-P, Epps CW, Carpenter LM (2007) How King et al. (2006)
1164 define an "evolutionary distinction" of a mouse subspecies: a response. *Molecular Ecology*,
1165 **16**, 3518–3521.

1166 Raymond M, Rousset F (1995) GENEPOP (version 1.2): population genetics software for exact
1167 tests and ecumenicism. *Journal of Heredity*, **86**, 248–249.

1168 Richardson JL, Brady SP, Wang IJ, Spear SF (2016) Navigating the pitfalls and promise of
1169 landscape genetics. *Molecular Ecology*, **25**, 849–863.

1170 Richardson JL, Urban MC, Bolnick DI, Skelly DK (2014) Microgeographic adaptation and the
1171 spatial scale of evolution. *Trends in Ecology & Evolution*, **29**, 165–179.

1172 Rousset F (2008) GENEPOP'007: A complete re-implementation of the GENEPOP software for
1173 Windows and Linux. *Molecular Ecology Resources*.

1174 Row JR, Blouin-Demers G, Lougheed SC (2010) Habitat distribution influences dispersal and
1175 fine-scale genetic population structure of eastern foxsnakes (Mintonius gloydi) across a
1176 fragmented landscape. *Molecular Ecology*, **19**, 5157–5171.

1177 Sawyer SC, Epps CW, Brashares JS (2011) Placing linkages among fragmented habitats: Do
1178 least-cost models reflect how animals use landscapes? *Journal of Applied Ecology*, **48**, 668–
1179 678.

1180 Schwartz MK, Copeland JP, Anderson NJ *et al.* (2009) Wolverine gene flow across a narrow
1181 climatic niche. *Ecology*, **90**, 3222–3232.

1182 Scribner KT, Blanchong JA, Bruggeman DJ *et al.* (2005) Geographical Genetics: Conceptual
1183 Foundations and Empirical Applications of Spatial Genetic Data in Wildlife Management.
1184 *The Journal of Wildlife Management*, **69**, 1434–1453.

1185 Segelbacher G, Cushman SA, Epperson BK *et al.* (2010) Application of landscapes genetics in
1186 conservation biology: concepts and challenges. *Conservation Genetics*, **11**, 375–385.

1187 Sexton JP, Hangartner SB, Hoffmann AA (2014) Genetic isolation by environment or distance:
1188 Which pattern of gene flow is most common? *Evolution*, **68**, 1–15.

1189 Shafer ABA, Northrup JM, White KS *et al.* (2012) Habitat selection predicts genetic relatedness
1190 in an alpine ungulate. *Ecology*, **93**, 1217–1329.

1191 Shaw WT (1934) The ability of the giant kangaroo rat as a harvester and storer of seeds. *Journal*

1192 *of Mammalogy*, **14**, 275–286.

1193 Shier DM, Lea AJ, Owen MA (2012) Beyond masking: Endangered Stephen's kangaroo rats
1194 respond to traffic noise with footdrumming. *Biological Conservation*, **150**, 53–58.

1195 Short Bull RA, Cushman SA, MacE R *et al.* (2011) Why replication is important in landscape
1196 genetics: American black bear in the Rocky Mountains. *Molecular Ecology*, **20**, 1092–1107.

1197 Skvarla JL, Nichols JD, Hines JE, Waser PM (2004) Modeling interpopulation dispersal by
1198 banner-tailed kangaroo rats. *Ecology*, **85**, 2737–2746.

1199 Smouse PE, Long JC, Sokal RR (1986) Multiple regression and correlation extensions of the
1200 mantel test of matrix correspondence. *Systematic Zoology*, **35**, 627–632.

1201 Smouse PE, Peakall R (1999) Spatial autocorrelation analysis of individual multiallele and
1202 multilocus genetic structure. *Heredity*, **82**, 561–573.

1203 Spear SF, Balkenhol N, Fortin M-J, McRae BH, Scribner K (2010) Use of resistance surfaces for
1204 landscape genetic studies: considerations for parameterization and analysis. *Molecular*
1205 *ecology*, **19**, 3576–91.

1206 Steinwald MC, Swanson BJ, Doyle JM, Waser PM (2013) Female mobility and the mating
1207 system of teh banner-tailed kangaroo rat (Dipodomys spectabilis). *Journal of Mammalogy*,
1208 **94**, 1258–1265.

1209 Storfer A, Murphy MA, Evans JS *et al.* (2007) Putting the "landscape" in landscape
1210 genetics. *Heredity*, **98**, 128–142.

1211 van Strien MJ, Holderegger R, Van Heck HJ (2015) Isolation-by-distance in landscapes:
1212 considerations for landscape genetics. *Heredity*, **114**, 27–37.

1213 Sunnucks P (2000) Efficient genetic markers for population biology. *Trends in Ecology and*
1214 *Evolution*, **15**, 199–203.

1215 Thibault KM, Ernest SKM, White EP, Brown JH, Jacob R (2010) Long-term insights into the
1216 influence of precipitation on community dynamics in desert rodents. *Journal of*
1217 *Mammalogy*, **91**, 787–797.

1218 Trumbo DR, Spear SF, Baumsteiger J, Storfer A (2013) Rangewide landscape genetics of an
1219 endemic Pacific northwestern salamander. *Molecular Ecology*, **22**, 1250–1266.

1220 Turchin P (1998) *Quantitative analysis of movement measuring and modeling population*
1221 *redistribution in animals and plants*. Sinauer Associates, Inc., Sunderland, Massachusetts.

1222 U. S. Census Bureau (2008a) *TIGER lines-San Benito County, CA*.

1223 U. S. Census Bureau (2008b) *TIGER lines-Fresno County, CA*.

1224 U. S. Geological Survey (2006) *Shuttle Radar Topography Mission*. College Park, Maryland.

1225 U. S. Geological Survey (2014) *Data Basin Database*.

1226 U.S. Forest Service (2010) *Remote Sensing Lab*. Sacramento, CA.

1227 Valone TJ, Brown JH, Jacobi CL (1995) Catastrophic Decline Of A Desert Rodent, Dipodomys
1228 Spectabilis - Insights From A Long-Term Study. *Journal Of Mammalogy*, **76**, 428–436.

1229 Wahlund S (1928) Zusammensetzung von populationen und korrelationserscheinungen vom
1230 standpunkt der vererbungslehre aus betrachtet. *Hereditas*, **11**, 65–106.

1231 Waits LP, Cushman SA, Spear SF (2016) Applications of landscape genetics to connectivity
1232 research in terrestrial animals. In: *Landscape genetics: concepts, methods, applications* (eds
1233 Balkenhol N, Cushman SA, Storfer A, Waits LP), pp. 199–214. Wiley, West Sussex, UK.

1234 Waits LP, Storfer A (2016) Basics of population genetics: quantifying neutral and adaptive
1235 genetic variation for landscape studies. In: *Landscape genetics: concepts, methods,*
1236 *applications* (eds Balkenhol N, Cushman SA, Storfer A, Waits LP), pp. 35–53. Wiley, West
1237 Sussex, UK.

1238 Wang J (2004) Sibship reconstruction from genetic data with typing errors. *Genetics*, **166**, 1963–
1239 1979.

1240 Wang IJ (2010) Recognizing the temporal distinctions between landscape genetics and
1241 phylogeography. *Molecular Ecology*, **19**, 2605–2608.

1242 Wang J (2012) Computationally efficient sibship and parentage assignment from multilocus
1243 marker data. *Genetics*, **191**, 183–194.

1244 Wang J (2016) User's guide for software COLONY version 2.0.6.1. , **1**, 1–70.

1245 Wang IJ, Summers K (2010) Genetic structure is correlated with phenotypic divergence rather
1246 than geographic isolation in the highly polymorphic strawberry poison-dart frog. *Molecular*
1247 *Ecology*, **19**, 447–458.

1248 Wang YH, Yang KC, Bridgman CL, Lin LK (2008) Habitat suitability modelling to correlate
1249 gene flow with landscape connectivity. *Landscape Ecology*, **23**, 989–1000.

1250 Waples RS (2015) Testing for Hardy-Weinberg proportions: have we lost the plot? *Heredity*,
1251 **106**, 1–19.

1252 Waples RS, Gaggiotti O (2006) What is a population? An empirical evaluation of some genetic
1253 methods for identifying the number of gene pools and their degree of connectivity.
1254 *Molecular Ecology*, **15**, 1419–1439.

1255 Warren DL, Glor RE, Turelli M (2010) ENMTools: A toolbox for comparative studies of
1256 environmental niche models. *Ecography*, **33**, 607–611.

1257 Warren DL, Seifert SN (2011) Ecological niche modeling in Maxent: the importance of model
1258 complexity and the performance of model selection criteria. *Ecological Applications*, **21**,
1259 335–342.

1260 Wasserman TN, Cushman SA, Schwartz MK, Wallin DO (2010) Spatial scaling and multi-model
1261 inference in landscape genetics:Martes americana in northern Idaho. *Landscape Ecology*,

25, 1601–1612.

Williams DF, Kilburn KS (1991) Dipodomys ingens. *Mammalian Species*, **377**, 1–7.

Womble WH (1951) Differential systematics. *Science*, **114**, 315–322.

Yannic G, Pellisier L, Le Corre M *et al.* (2014) Temporally dynamic habitat suitability predicts relatedness among caribou. *Proceedings of the Royal Society B*, **281**, 20140502.

Zeller KA, Creech TG, Millette KL *et al.* (2016) Using simulations to evaluate Mantel-based methods for assessing landscape resistance to gene flow. *Ecology and Evolution*.

Zeller KA, McGarigal K, Whiteley AR (2012) Estimating landscape resistance to movement: a review. *Landscape Ecology*, **27**, 777–797.

Appendices

Appendix A: The cost assignments of vegetation communities used in the additive models and the parameterization of Veg Multi, and the cost assignment of roads used for additive models

Vegetation Community	Cost Assignment
Barren	0.001
Pasture	0.1
Grassland	0.2
Chaparral	0.3
Scrub	0.3
Sagebrush	0.3
Alkali Desert Scrub	0.3
Crop	0.4
Orchard	0.5
Oak	0.6
Hardwood	0.6
Irrigated Row Crop	0.7
Riparian	0.8
Wet Meadow	0.8
Urban	1
Lacustrine	1
Riverine	1
Roads	
Road Present	0
Road Absent	0.3

Appendix B: Maxent model selection table used to determine the habitat suitability model used as a resistance and conductance (bold) with the included parameters, smoothing coefficient (Beta), log likelihood, number of parameters, and the Akiake's Information Criterion corrected for small sample size

Included Parameters	Beta	Log Likelihood	Number of Parameters	AICc score
Precipitation Slope Vegetation Roads	**1**	**-6349.56825**	**26**	**12754.1365**
Precipitation Slope Vegetation	1	-6383.948395	26	12822.89679
Slope Vegetation Roads	1	-6416.257738	23	12880.85942
Precipitation Slope Vegetation Roads	2	-6425.021599	23	12898.38715
Precipitation Slope Vegetation Roads	3	-6463.876376	15	12958.75484
Slope Vegetation	1	-6461.865782	17	12959.01458
Slope Vegetation Roads	2	-6478.844967	21	13001.64342
Precipitation Slope Vegetation	2	-6486.356439	18	13010.14985
Precipitation Slope Vegetation Roads	4	-6503.561497	16	13040.26107
Precipitation Slope Roads	1	-6511.655158	18	13060.74729
Slope Vegetation	2	-6523.554764	16	13080.2476
Slope Vegetation Roads	3	-6534.261241	15	13099.52457
Precipitation Slope Roads	2	-6546.273837	14	13121.42267
Slope Vegetation Roads	4	-6549.786422	12	13124.22015
Precipitation Slope	1	-6555.672142	18	13148.78126
Slope Vegetation	3	-6566.310566	10	13153.07568
Precipitation Slope Roads	3	-6569.017023	11	13160.58063
Precipitation Slope Vegetation	3	-6566.273701	15	13163.54949
Precipitation Slope Roads	4	-6576.681869	9	13171.73487
Slope Vegetation	4	-6591.563308	10	13203.58116
Precipitation Slope Vegetation	4	-6593.958147	12	13212.5636
Precipitation Slope	2	-6599.725793	12	13224.09889
Precipitation Slope	3	-6638.91782	9	13296.20677
Slope Roads	1	-6648.407126	16	13329.95233
Slope Roads	2	-6678.890655	12	13382.42861
Precipitation Slope	4	-6685.458807	10	13391.37216
Slope Roads	3	-6687.247393	10	13394.94933
Slope Roads	4	-6700.181626	6	13412.53538
Precipitation Vegetation Roads	1	-6732.858193	16	13498.85446
Precipitation Vegetation	1	-6778.190487	12	13581.02828
Precipitation Vegetation Roads	2	-6805.955616	13	13638.66799
Vegetation Roads	1	-6818.080834	10	13656.61621
Precipitation Vegetation Roads	3	-6841.778298	10	13704.01114
Precipitation Roads	1	-6852.477739	6	13717.12761
Precipitation Vegetation Roads	4	-6854.848112	8	13725.99252
Precipitation Vegetation	2	-6854.868562	14	13738.61212

Included Parameters	Beta	Log Likelihood	Number of Parameters	AICc score
Precipitation Roads	2	-6867.098243	6	13746.36862
Vegetation Roads	2	-6867.100892	13	13760.95854
Precipitation Roads	3	-6881.030853	5	13772.18441
Precipitation Roads	4	-6898.979281	5	13808.08126
Vegetation Roads	3	-6902.4123	6	13816.99673
Vegetation Roads	4	-6912.51243	5	13835.14756
Precipitation Vegetation	3	-6912.659426	6	13837.49098
Precipitation Vegetation	4	-6945.901249	4	13899.88413

Appendix C: Individual assignment probabilities to a discrete population with confidence intervals from a single k=4 STRUCTURE run

Individual ID	Pop 1	Pop 2	Pop 3	Pop 4	Pop 1 CI	Pop 2 CI	Pop 3 CI	Pop 4 CI
K-0002	0.01	0.06	0.64	0.29	(0, 0.15)	(0, 0.72)	(0, 1)	(0, 1)
K-0005	0.01	0.03	0.71	0.25	(0, 0.14)	(0, 0.31)	(0, 1)	(0, 1)
K-0008	0.05	0.03	0.72	0.2	(0, 0.52)	(0, 0.35)	(0, 1)	(0, 1)
K-0011	0.01	0.07	0.91	0.01	(0, 0.09)	(0, 0.99)	(0, 1)	(0, 0.13)
K-0014	0.01	0.06	0.93	0.01	(0, 0.1)	(0, 1)	(0, 1)	(0, 0.07)
K-0021	0.01	0.02	0.79	0.18	(0, 0.14)	(0, 0.25)	(0, 1)	(0, 1)
K-0022	0.01	0.01	0.76	0.23	(0, 0.11)	(0, 0.11)	(0, 1)	(0, 1)
K-0023	0.01	0.04	0.83	0.11	(0, 0.17)	(0, 0.47)	(0, 1)	(0, 1)
K-0024	0.01	0.05	0.92	0.01	(0, 0.14)	(0, 0.99)	(0, 1)	(0, 0.14)
K-0025	0.02	0.07	0.9	0.02	(0, 0.18)	(0, 0.98)	(0, 1)	(0, 0.18)
K-0026	0.02	0.07	0.9	0.01	(0, 0.24)	(0, 1)	(0, 1)	(0, 0.15)
K-0027	0.01	0.92	0.05	0.01	(0, 0.12)	(0, 1)	(0, 1)	(0, 0.15)
K-0028	0.08	0.09	0.68	0.15	(0, 0.61)	(0, 0.97)	(0, 1)	(0, 1)
K-0029	0.03	0.02	0.77	0.18	(0, 0.33)	(0, 0.25)	(0, 1)	(0, 1)
K-0030	0.07	0.91	0.02	0.01	(0, 0.89)	(0, 1)	(0, 0.16)	(0, 0.07)
K-0031	0.31	0.59	0.08	0.02	(0, 1)	(0, 1)	(0, 0.95)	(0, 0.27)
K-0032	0.01	0.71	0.16	0.13	(0, 0.13)	(0, 1)	(0, 1)	(0, 1)
K-0033	0.01	0.91	0.06	0.02	(0, 0.07)	(0, 1)	(0, 0.99)	(0, 0.24)
K-0034	0.14	0.25	0.22	0.39	(0, 0.79)	(0, 1)	(0, 1)	(0, 1)
K-0036	0.01	0.62	0.08	0.29	(0, 0.16)	(0, 1)	(0, 0.98)	(0, 1)
K-0037	0.01	0.01	0.01	0.98	(0, 0.09)	(0, 0.07)	(0, 0.09)	(0.82, 1)
K-0038	0.04	0.28	0.05	0.62	(0, 0.42)	(0, 1)	(0, 0.97)	(0, 1)
K-0039	0.01	0.68	0.07	0.24	(0, 0.16)	(0, 1)	(0, 0.99)	(0, 1)
K-0040	0.03	0.82	0.09	0.07	(0, 0.3)	(0, 1)	(0, 1)	(0, 0.8)
K-0041	0.09	0.89	0.02	0.01	(0, 0.93)	(0, 1)	(0, 0.16)	(0, 0.07)
K-0042	0.89	0.07	0.02	0.03	(0.33, 1)	(0, 0.59)	(0, 0.18)	(0, 0.33)
K-0043	0.03	0.88	0.07	0.02	(0, 0.37)	(0, 1)	(0, 0.99)	(0, 0.2)
K-0044	0.03	0.02	0.05	0.91	(0, 0.35)	(0, 0.16)	(0, 0.97)	(0, 1)
K-0045	0.07	0.59	0.29	0.04	(0, 0.98)	(0, 1)	(0, 1)	(0, 0.64)
K-0046	0.01	0.3	0.6	0.09	(0, 0.11)	(0, 1)	(0, 1)	(0, 0.99)
K-0047	0.02	0.89	0.07	0.02	(0, 0.22)	(0, 1)	(0, 0.96)	(0, 0.19)
K-0048	0.05	0.21	0.08	0.66	(0, 0.47)	(0, 1)	(0, 0.97)	(0, 1)
K-0049	0.01	0.02	0.03	0.94	(0, 0.1)	(0, 0.27)	(0, 0.34)	(0.5, 1)
K-0051	0.03	0.03	0.27	0.67	(0, 0.36)	(0, 0.34)	(0, 1)	(0, 1)
K-0052	0.01	0.03	0.18	0.78	(0, 0.16)	(0, 0.29)	(0, 1)	(0, 1)
K-0053	0.01	0.02	0.01	0.96	(0, 0.11)	(0, 0.17)	(0, 0.15)	(0.69, 1)
K-0054	0.03	0.92	0.03	0.02	(0, 0.3)	(0.36, 1)	(0, 0.42)	(0, 0.25)
K-0055	0.01	0.03	0.08	0.89	(0, 0.07)	(0, 0.33)	(0, 0.98)	(0, 1)
K-0056	0.01	0.01	0.04	0.95	(0, 0.07)	(0, 0.11)	(0, 0.34)	(0.63, 1)

Individual ID	Pop 1	Pop 2	Pop 3	Pop 4	Pop 1 CI	Pop 2 CI	Pop 3 CI	Pop 4 CI
K-0057	0.04	0.44	0.38	0.14	(0, 0.38)	(0, 1)	(0, 1)	(0, 1)
K-0058	0.01	0.91	0.06	0.02	(0, 0.13)	(0, 1)	(0, 0.99)	(0, 0.24)
K-0059	0.01	0.97	0.02	0.01	(0, 0.09)	(0.75, 1)	(0, 0.17)	(0, 0.08)
K-0061	0.01	0.94	0.04	0.02	(0, 0.13)	(0.06, 1)	(0, 0.8)	(0, 0.19)
K-0062	0.02	0.03	0.12	0.83	(0, 0.24)	(0, 0.37)	(0, 1)	(0, 1)
K-0064	0.01	0.44	0.06	0.49	(0, 0.11)	(0, 1)	(0, 0.81)	(0, 1)
K-0065	0.01	0.3	0.15	0.54	(0, 0.12)	(0, 1)	(0, 1)	(0, 1)
K-0066	0.02	0.89	0.05	0.03	(0, 0.26)	(0, 1)	(0, 0.85)	(0, 0.35)
K-0067	0.09	0.83	0.05	0.03	(0, 0.75)	(0, 1)	(0, 0.78)	(0, 0.36)
K-0068	0.1	0.84	0.04	0.02	(0, 0.79)	(0, 1)	(0, 0.82)	(0, 0.18)
K-0069	0.01	0.02	0.01	0.96	(0, 0.17)	(0, 0.17)	(0, 0.13)	(0.67, 1)
K-0070	0.1	0.58	0.27	0.06	(0, 0.99)	(0, 1)	(0, 1)	(0, 0.71)
K-0071	0.12	0.49	0.38	0.02	(0, 0.75)	(0, 1)	(0, 1)	(0, 0.2)
K-0072	0.04	0.04	0.49	0.44	(0, 0.41)	(0, 0.42)	(0, 1)	(0, 1)
K-0073	0.04	0.01	0.13	0.82	(0, 0.44)	(0, 0.14)	(0, 1)	(0, 1)
K-0074	0.03	0.03	0.06	0.87	(0, 0.4)	(0, 0.4)	(0, 0.97)	(0, 1)
K-0075	0.08	0.76	0.09	0.07	(0, 0.65)	(0, 1)	(0, 0.99)	(0, 0.85)
K-0076	0.01	0.96	0.03	0.01	(0, 0.1)	(0.64, 1)	(0, 0.29)	(0, 0.08)
K-0078	0.01	0.94	0.05	0.01	(0, 0.08)	(0, 1)	(0, 0.98)	(0, 0.13)
K-0079	0.04	0.01	0.17	0.78	(0, 0.47)	(0, 0.13)	(0, 1)	(0, 1)
K-0080	0.01	0.65	0.3	0.04	(0, 0.12)	(0, 1)	(0, 1)	(0, 0.54)
K-0081	0.02	0.59	0.33	0.06	(0, 0.21)	(0, 1)	(0, 1)	(0, 0.9)
K-0082	0.19	0.02	0.05	0.74	(0, 0.89)	(0, 0.16)	(0, 0.82)	(0, 1)
K-0083	0.92	0.01	0.04	0.03	(0.46, 1)	(0, 0.15)	(0, 0.39)	(0, 0.37)
K-0084	0.9	0.03	0.03	0.04	(0.4, 1)	(0, 0.29)	(0, 0.32)	(0, 0.45)
K-0085	0.86	0.02	0.05	0.07	(0.29, 1)	(0, 0.27)	(0, 0.45)	(0, 0.51)
K-0086	0.92	0.03	0.04	0.02	(0.48, 1)	(0, 0.28)	(0, 0.44)	(0, 0.19)
K-0087	0.98	0.01	0.01	0.01	(0.84, 1)	(0, 0.07)	(0, 0.09)	(0, 0.07)
K-0088	0.02	0.04	0.07	0.87	(0, 0.27)	(0, 0.54)	(0, 0.85)	(0, 1)
K-0090	0.98	0.01	0.01	0.01	(0.82, 1)	(0, 0.09)	(0, 0.1)	(0, 0.09)
K-0091	0.94	0.03	0.02	0.01	(0.54, 1)	(0, 0.34)	(0, 0.18)	(0, 0.17)
K-0092	0.95	0.02	0.02	0.01	(0.63, 1)	(0, 0.19)	(0, 0.25)	(0, 0.13)
K-0093	0.96	0.01	0.01	0.02	(0.69, 1)	(0, 0.12)	(0, 0.14)	(0, 0.22)
K-0094	0.53	0.23	0.16	0.08	(0, 1)	(0, 1)	(0, 0.92)	(0, 0.62)
K-0095	0.04	0.09	0.72	0.16	(0, 0.38)	(0, 1)	(0, 1)	(0, 1)
K-0096	0.98	0.01	0.01	0.01	(0.86, 1)	(0, 0.07)	(0, 0.06)	(0, 0.06)
K-0097	0.01	0.04	0.82	0.13	(0, 0.12)	(0, 0.5)	(0, 1)	(0, 1)
K-0098	0.01	0.08	0.36	0.55	(0, 0.17)	(0, 0.94)	(0, 1)	(0, 1)
K-0099	0.95	0.02	0.01	0.01	(0.63, 1)	(0, 0.26)	(0, 0.16)	(0, 0.17)
K-0100	0.36	0.18	0.42	0.05	(0, 1)	(0, 1)	(0, 1)	(0, 0.57)
K-0101	0.97	0.01	0.01	0.01	(0.72, 1)	(0, 0.08)	(0, 0.17)	(0, 0.17)
K-0102	0.91	0.01	0.02	0.06	(0.25, 1)	(0, 0.13)	(0, 0.17)	(0, 0.68)

Individual ID	Pop 1	Pop 2	Pop 3	Pop 4	Pop 1 CI	Pop 2 CI	Pop 3 CI	Pop 4 CI
K-0103	0.96	0.01	0.01	0.01	(0.71, 1)	(0, 0.16)	(0, 0.14)	(0, 0.14)
K-0104	0.87	0.03	0.03	0.07	(0.35, 1)	(0, 0.36)	(0, 0.29)	(0, 0.56)
K-0105	0.98	0.01	0.01	0.01	(0.85, 1)	(0, 0.06)	(0, 0.06)	(0, 0.09)
K-0106	0.04	0.23	0.3	0.43	(0, 0.47)	(0, 1)	(0, 1)	(0, 1)
K-0107	0.96	0.01	0.01	0.02	(0.68, 1)	(0, 0.16)	(0, 0.11)	(0, 0.26)
K-0108	0.08	0.07	0.07	0.78	(0, 0.62)	(0, 0.74)	(0, 0.95)	(0, 1)
K-0109	0.1	0.05	0.05	0.8	(0, 0.65)	(0, 0.52)	(0, 0.91)	(0, 1)
K-0110	0.07	0.05	0.05	0.83	(0, 0.72)	(0, 0.72)	(0, 0.84)	(0, 1)
K-0111	0.05	0.02	0.04	0.89	(0, 0.59)	(0, 0.25)	(0, 0.86)	(0, 1)
K-0112	0.02	0.02	0.09	0.87	(0, 0.2)	(0, 0.27)	(0, 1)	(0, 1)
K-0113	0.02	0.1	0.15	0.73	(0, 0.19)	(0, 1)	(0, 1)	(0, 1)
K-0117	0.03	0.03	0.1	0.85	(0, 0.33)	(0, 0.33)	(0, 1)	(0, 1)
K-0153	0.03	0.48	0.09	0.39	(0, 0.35)	(0, 1)	(0, 1)	(0, 1)
K-0155	0.02	0.79	0.09	0.1	(0, 0.26)	(0, 1)	(0, 1)	(0, 0.98)
K-0156	0.47	0.02	0.04	0.47	(0, 1)	(0, 0.22)	(0, 0.57)	(0, 1)
K-0158	0.01	0.39	0.11	0.49	(0, 0.12)	(0, 1)	(0, 1)	(0, 1)
K-0159	0.02	0.78	0.07	0.12	(0, 0.27)	(0, 1)	(0, 1)	(0, 1)
K-0160	0.01	0.75	0.09	0.15	(0, 0.16)	(0, 1)	(0, 1)	(0, 1)
K-0161	0.19	0.55	0.05	0.2	(0, 1)	(0, 1)	(0, 0.85)	(0, 1)
K-0162	0.4	0.07	0.09	0.44	(0, 1)	(0, 0.83)	(0, 0.96)	(0, 1)
K-0163	0.02	0.83	0.12	0.03	(0, 0.26)	(0, 1)	(0, 1)	(0, 0.33)
K-0167	0.01	0.04	0.06	0.89	(0, 0.09)	(0, 0.51)	(0, 0.81)	(0, 1)
K-0170	0.01	0.03	0.05	0.91	(0, 0.12)	(0, 0.37)	(0, 0.52)	(0.32, 1)
K-0171	0.01	0.05	0.92	0.03	(0, 0.09)	(0, 0.99)	(0, 1)	(0, 0.28)
K-0175	0.06	0.05	0.15	0.74	(0, 0.52)	(0, 0.57)	(0, 1)	(0, 1)
K-0177	0.26	0.18	0.12	0.44	(0, 1)	(0, 1)	(0, 1)	(0, 1)
K-0179	0.03	0.6	0.33	0.04	(0, 0.35)	(0, 1)	(0, 1)	(0, 0.51)
K-0182	0.01	0.04	0.91	0.04	(0, 0.06)	(0, 0.99)	(0, 1)	(0, 0.91)
K-0189	0.11	0.04	0.03	0.82	(0, 0.63)	(0, 0.57)	(0, 0.33)	(0, 1)
K-0197	0.01	0.02	0.05	0.93	(0, 0.11)	(0, 0.21)	(0, 0.62)	(0.24, 1)
K-0198	0.02	0.92	0.05	0.02	(0, 0.19)	(0, 1)	(0, 0.9)	(0, 0.17)
K-0199	0.01	0.69	0.29	0.02	(0, 0.1)	(0, 1)	(0, 1)	(0, 0.18)
K-0202	0.09	0.8	0.07	0.03	(0, 0.77)	(0, 1)	(0, 1)	(0, 0.39)
K-0204	0.01	0.75	0.07	0.18	(0, 0.06)	(0, 1)	(0, 1)	(0, 1)
K-0206	0.91	0.02	0.05	0.03	(0.48, 1)	(0, 0.2)	(0, 0.41)	(0, 0.32)
K-0211	0.11	0.05	0.04	0.81	(0, 0.94)	(0, 0.7)	(0, 0.41)	(0, 1)
K-0214	0.05	0.19	0.04	0.72	(0, 0.51)	(0, 1)	(0, 0.46)	(0, 1)
K-0219	0.02	0.02	0.05	0.91	(0, 0.24)	(0, 0.24)	(0, 0.54)	(0.09, 1)
K-0230	0.01	0.86	0.11	0.02	(0, 0.13)	(0, 1)	(0, 1)	(0, 0.19)
K-0234	0.02	0.03	0.83	0.12	(0, 0.24)	(0, 0.41)	(0, 1)	(0, 1)
K-0060	0.15	0.1	0.07	0.69	(0, 1)	(0, 0.97)	(0, 0.99)	(0, 1)
K-0143	0.2	0.17	0.08	0.55	(0, 1)	(0, 1)	(0, 1)	(0, 1)

Appendix D: Population size (N), mean allelic richness (N_A), number of private alleles, inbreeding coefficient (F_{IS}; 1-Ho/He), observed heterozygosity (Ho) and expected heterozygosity (He) across the study area and for each population identified by Tess and STRUCTURE with means ± the standard error

	N	N_A	Private alleles	F_{IS}	Ho	He
Total	120.86 ± 0.1	14.36 ± 1.05	na	0.11 ± 0.02	0.73 ± 0.04	0.82 ± 0.04
TESS						
Panoche Valley	82 ± 0	13.5 ± 1.02	25	0.1 ± 0.02	0.74 ± 0.04	0.82 ± 0.04
Tumey Hills	16.86 ± 0.1	9.57 ± 0.66	3	0.16 ± 0.05	0.64 ± 0.05	0.78 ± 0.04
Ciervo Hills	22 ± 0	10.64 ± 0.77	6	0.05 ± 0.04	0.75 ± 0.04	0.8 ± 0.04
STRUCTURE						
Panoche Valley	41 ± 0	12.79 ± 0.84	13	0.06 ± 0.03	0.77 ± 0.04	0.82 ± 0.04
Panoche Hills	22 ± 0	10.5 ± 0.73	2	0.11 ± 0.04	0.73 ± 0.04	0.82 ± 0.03
Tumey Hills	38.86 ± 0.1	11.71 ± 0.82	11	0.13 ± 0.03	0.71 ± 0.04	0.81 ± 0.04
Ciervo Hills	19 ± 0	8.29 ± 0.72	1	0.07 ± 0.04	0.7 ± 0.06	0.75 ± 0.05